Research and Technology

Annual Report 1983

Lewis Research Center

NASA Technical Memorandum 83540

NASA
National Aeronautics and Space Administration

Contents

Introduction

This report presents highlights of the research accomplishments of the Lewis Research Center for fiscal year 1983. It is the seventh annual report in this series. The report is divided into four major sections covering aeronautics, spaceflight, space technology, and materials and structures. Each section contains descriptions of work in both basic research and technology activities and in project activities.

Products of Lewis' research, used in both commercial and military aircraft and in space vehicles, have helped maintain the United States' position in these fields. Lewis' research is also contributing to the improved efficiency of current energy conversion systems and to the development of hardware and systems designed to make use of alternative energy sources.

This report describes 78 Lewis research projects that produced significant results. The results of all research and technology work performed during the fiscal year are contained in 733 Lewis-published technical reports and presentations prepared either by Lewis scientists and engineers or by contractor personnel.

An additional highlight of 1983 is that four Lewis products were selected for the Industrial Research & Development magazine's IR-100 Awards. One of the awards, for a "New Silicon Carbide Crystal Growth Process," was given solely to Lewis. The other three awards, for a "System for High-Speed Balancing of Shafts," "High-Frequency, High-Power Capacitor," and "High-Speed Switch Matrix for Advanced Communications Systems" were shared jointly by Lewis and the several contractors who were codevelopers. All of the work that received an award is described in this report.

For general information about the report, contact Robert Finkelstein at (216) 433-4000, Ext. 706, or FTS 294-6706.

Aeronautics

Highly Maneuverable Supersonic Inlets

Mission studies indicate that the next generation of supersonic tactical aircraft will require greater subsonic and transonic maneuverability than current aircraft. The aircraft may be required to operate at an angle of attack of 45° and an angle of yaw of 15° while at a Mach number of 0.9. At these severe operating conditions the inlet must supply the engine with high-pressure, low-distortion air to ensure high thrust levels and satisfactory inlet-engine compatibility.

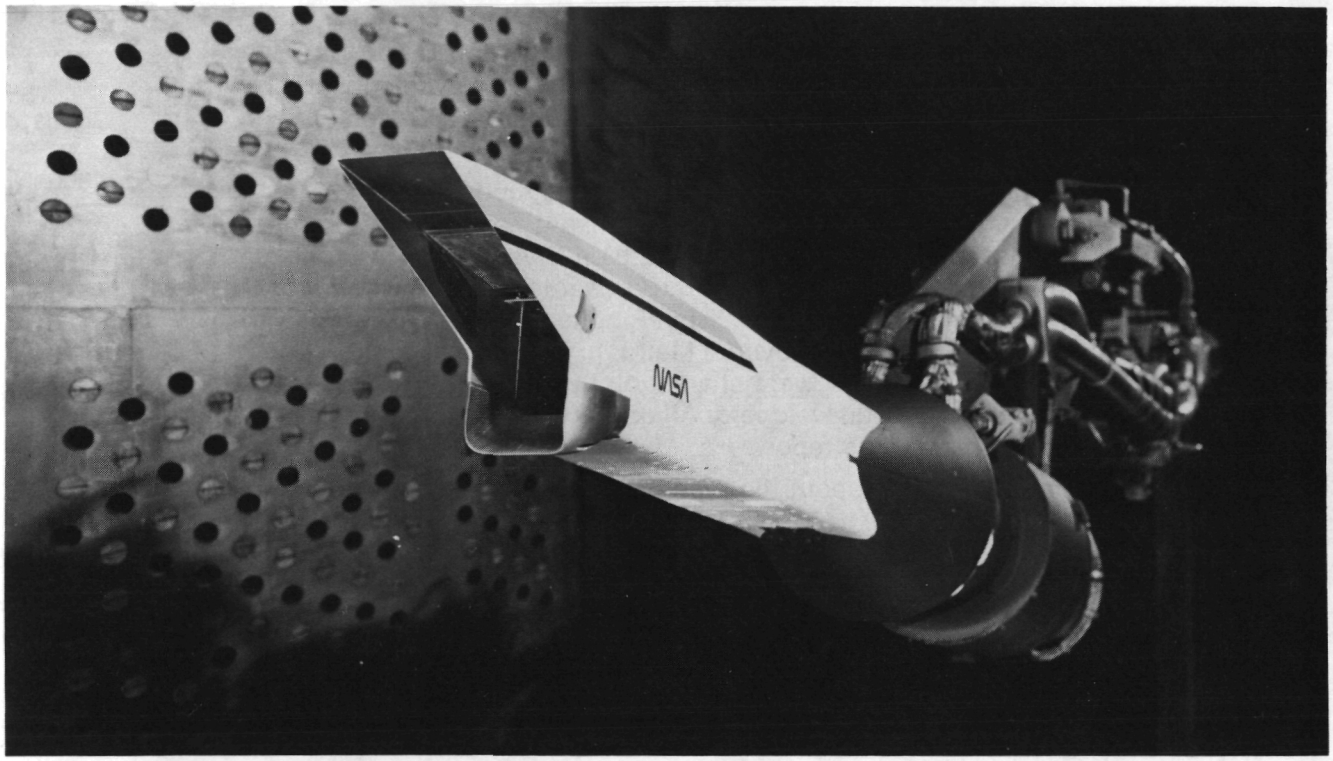

Two-dimensional supersonic inlet with drooping lower lip

A cooperative research program between Lewis and the McDonnell Aircraft Company was initiated to investigate methods for providing acceptable inlet performance at these conditions. Tests were conducted in the Lewis 8- by 6-Foot Supersonic Wind Tunnel with inlet models provided by McDonnell. Both axisymmetric and two-dimensional supersonic inlets were tested.

Test results indicated that drooping the inlet lower lip would significantly improve inlet performance. For example, at Mach 0.9 and an angle of attack of 40°, drooping the inlet lower lip by 20° increased the efficiency of the axisymmetric inlet from 73 percent to 88 percent.

The efficiency of the two-dimensional inlet was also improved from 94 percent to 99 percent. These significant improvements suggest that the drooping lower lip is an attractive method for improving the inlet performance of future highly maneuverable tactical aircraft.

Scientific Research Associates and Lewis solves the entire Navier-Stokes equation in three dimensions, neglecting only the streamwise diffusion terms. The resulting finite-difference code (PEPSIS) solves for the flow in a plane normal to the stream direction by using a high-speed solver. The solution proceeds from plane to plane through the length of the inlet, incorporating special logic for subsonic and small recirculating regions of flow. A number of different boundary conditions and turbulence models are available to the user and a boundary layer bleed model is currently being verified. The

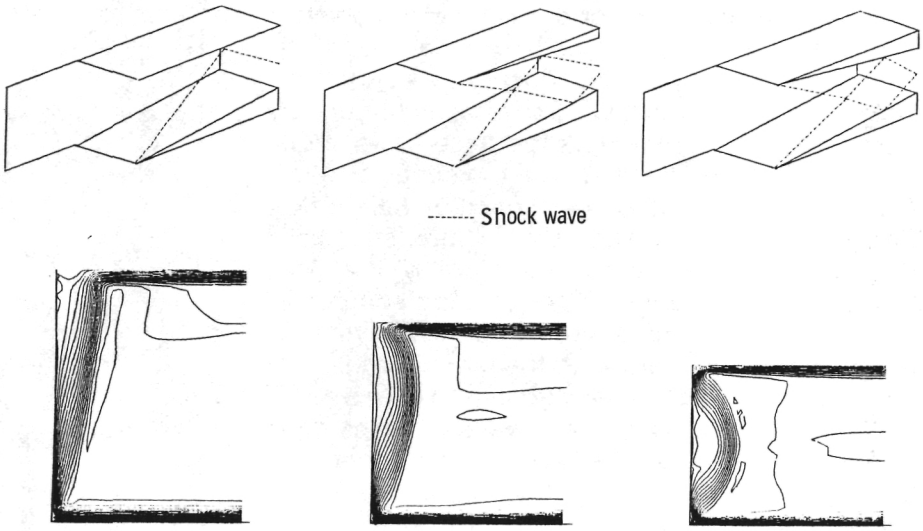

Downstream total pressure contours

Three-Dimensional Viscous Marching Analysis for Supersonic Inlets

Classical analysis of supersonic inlets involves an inviscid flow calculation with a correction for viscous effects. A new method developed by

code has been installed on the Cray 1 computer at Lewis and is being used for both analyzing and designing axisymmetric and rectangular supersonic inlets.

The PEPSIS code has recently been applied to three simple rectangular inlet configurations to study the glancing side-wall shock-boundary layer interaction present in this type of inlet. The results of these calculations indicate that the glancing shock sweeps the low-energy boundary layer flow along with it. For the case of a single

wedge and shock, this low-energy flow is swept into the corner of the cowl and side wall, and the streamwise pressure gradient of the shock reflection often causes flow separation and recirculation. For the cases with opposed wedge surfaces and multiple shocks, the low-energy flow is swept to near the center of the side wall and there is no indication of separation at the shock reflections. This basic information will aid in the design of efficient high-speed inlets.

Three-Dimensional Viscous Marching Analysis for Subsonic Internal Flow

Modern airbreathing propulsion systems often include subsonic inlets or diffusers with curved centerlines and varying cross-sectional shape that generate complex secondary flows and significant flow distortion. Conventional boundary layer analyses will not work for these flows, and full Navier-Stokes methods are too costly to use routinely. A new method developed by Scientific Research Associates and Lewis computes these flows by solving an approximate form of the Navier-Stokes equations. The resulting computer code (PEPSIG) solves the problem by marching from plane to plane through the length of the duct. Special logic is used for small regions of recirculating flow. The current version of the code has been installed on the Cray 1 computer at Lewis, and an extensive verification process is under way.

The PEPSIG code has recently been applied to a configuration approximating the B1 inlet. The duct has a curved centerline and a cross section that varies from nearly rectangular at the entrance to circular at the compressor face. The calculation was made for an entrance Mach number of 0.5 and a Reynolds number per foot of 1 million. Contours of constant total pressure and secondary flow pattern at the compressor face station show the distortion in the total pressure caused by the secondary flow. Calculations like these will aid in the basic understanding of complex three-dimensional internal flows and in the design of efficient subsonic inlets and diffusers.

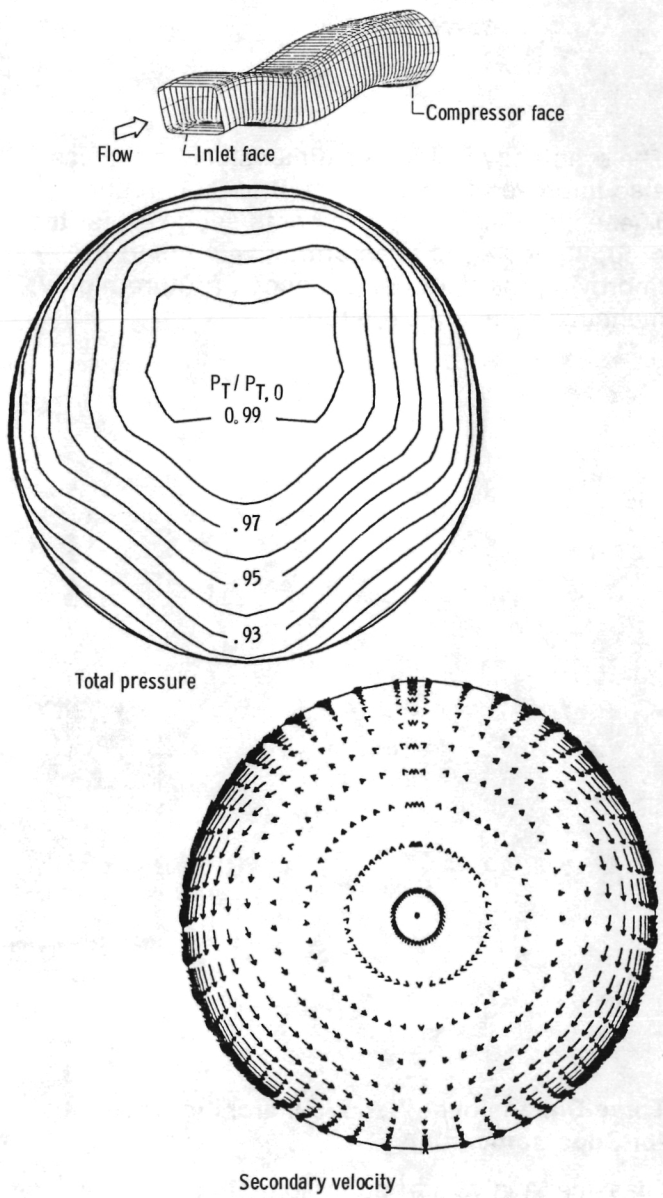

B1B inlet duct compressor face station

Fundamental Flame Radiation Measurements

A series of combustor tests were conducted with a tubular-can combustor to study flame radiation characteristics and effects with parametric variations in combustor operating conditions. Flame radiation was measured with a spectral radiance sensing instrument and with three total radiant heat flux transducers to expand the fundamental flame radiation data base for assessing the effect of radiative heat transfer to combustor liner walls. Data were obtained with Jet A fuel and ERBS (reduced hydrogen content) fuel. The data may lead to more durable combustor liners because advances in thermal analysis aid adjustments to liner cooling airflow distribution that optimize liner cooling efficiency. Thus liner development costs can be reduced by minimizing design iterations.

For example, the increase in total radiant heat flux with higher combustor pressures and inlet temperatures suggests greater radiative heat load to the combustor liner. However, local liner temperatures actually were lower at high combustor pressures. This is attributed to a large increase in convective cooling at high combustor pressures, sufficient to offset the increased flame radiation and still reduce liner temperatures. Thus, these fundamental data show the necessity for improved thermal analysis to aid in the combustor design process.

In addition, the ERBS fuel data consistently indicated an additional increase in radiant heat flux and liner temperatures in each combustion zone as compared with the Jet A fuel data. Thus, these fundamental data also show the necessity to assess the effect of fuel quality variances (deficiencies) on liner durability and hence ultimately to determine the acceptable limits of combustor operation.

In summary, these fundamental flame radiation measurements are a significant contribution to the fundamental data base required for the long-range combustion research objective of obtaining predictive computer codes that the combustion industry can apply in their combustion design system.

IR-100
New Silicon Carbide Crystal Growth Process

Last year high-temperature (500° to 1000° C) electronics moved much closer to reality with the in-house development of a reproducible process for growing large-area cubic silicon carbide (SiC) single-crystal wafers. Recently, this process was selected as one of the top 100 technological developments for the last year by Industrial Research & Development magazine.

Among the many applications requiring high-temperature electronics are signal conditioning electronics and high-reliability control electronics for aircraft turbine engines. Silicon carbide semiconductor devices have the potential for satisfying these engine requirements.

During the last year the process has been improved to the point that cubic SiC single-crystal layers nearly 50 μm thick can be grown on standard silicon single-crystal wafers. Also, research into the growth process has yielded significant new information regarding the nature of this heteroepitaxial crystal growth.

High-Temperature Heat Flux Sensors

Two major goals in the design of gas turbine engine combustor liners are to increase durability and to minimize the amount of cooling air required. Design verification requires that certain critical measurements be made as directly and accurately as possible during development testing. Heat flux is one of these critical design parameters.

Under contract to Lewis, Pratt & Whitney Aircraft has developed three types of heat flux sensors: a Gardon gage, a laminated gage, and an embedded-thermocouple gage. All three gages have been designed, fabricated, calibrated, and tested. The principle of operation in each case is the measurement of the temperature difference across a thermal barrier due to the heat flow. These sensors measure the combined heat flux from both radiation and convection. A unique feature of these sensors is their use of the superalloy liner material as part of the temperature-difference measuring circuit. Further development will lead to sensors suitable for use on turbine blades and vanes.

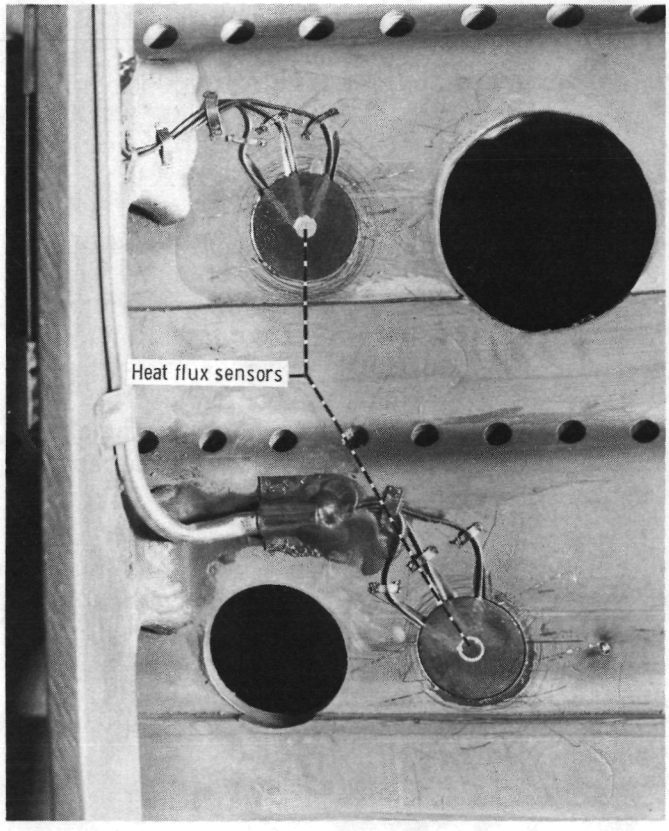

Combustor liner with heat flux sensors installed

Dynamic Gas Temperature-Measuring System

Fast-responding instruments are needed to measure the rapidly varying temperature of the hot gas exiting the combustor in a turbine engine. Knowledge of how the temperature varies with time can provide information about the combustion process and about the temperature fluctuations impcsed on the turbine blades and vanes.

The sensing probe used in this system has two thermocouples at a low frequency. It is possible to determine how to compensate the thermocouple signals to provide a measure of the fluctuating gas temperature over the frequency range of interest. The thermocouple signals are tape recorded and later processed on a digital computer after the engine test has been completed. The idea of compensating the signal from a sensor to achieve an extended frequency response is not new. However, in the case of temperature measurements in a gas stream, the

required compensation depends on the flow conditions. This system makes an onsite determination of the required compensation and thus accounts for the flow conditions.

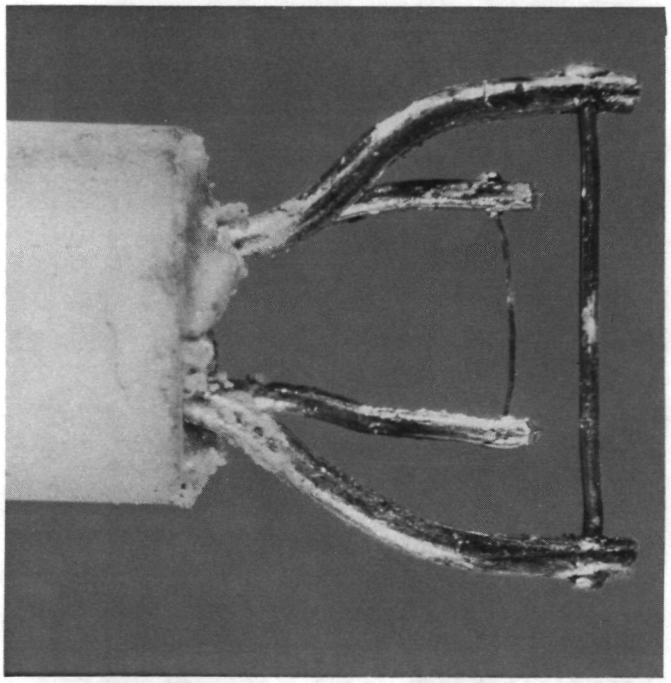

Dual-element dynamic gas temperature probe

Computer Code for Dilution Zone Mixing

The proper thermal conditioning of the products of combustion in gas turbine engines is accomplished by dilution with air. This process influences the average temperature level and uniformity of the gases leaving the combustor. The costly and time-consuming task of controlling or tailoring the exit temperature profiles through cut-and-try testing can be reduced with the aid of computer models capable of characterizing the exit distribution in terms of the upstream flow and geometric variables.

In its simplest geometry, the dilution process can be portrayed as jets penetrating normally into a straight duct flow. In 1972–75, Aerojet Liquid Rocket Company, under contract to Lewis, carried out an extensive experimental study of this configuration and developed an empirical model for predicting the temperature distributions. Recently, an interactive microcomputer code based on these correlations was developed at Lewis. This program allows the designer to investigate the effect of varying flow or geometric parameters and uses computer graphics to display two- and three-dimensional plots of the temperature profiles for any user-selected flow and geometry conditions.

The empirical-based code is fast; computer memory requirements are modest; and modification to use (and evaluate) new correlations is straightforward. The code provides an excellent predictive capability within the parameter range of the generating experiments.

Prediction of Turbine Inlet Temperature Profile Distortion

The large radial temperature variations produced by the combustor in a gas turbine engine result in nonuniform turbine inlet temperature profiles. A three-dimensional Euler code has been used to predict inlet temperature profile distortion within an axial turbine stage due to convection by secondary flow. Relative gas temperature rises of 40 to 95 deg K for a 670 K mean inlet temperature were predicted at the trailing-edge hub and tip corners on the pressure surfaces of both the stator and the rotor. Such redistributions of hot

gas cause hot spots on the blade and endwall surfaces that can invalidate assumptions made in the design of the cooling scheme and, hence, dramatically reduce the durability of the turbine.

Flutter Characteristics from Stationary Pressure Transducers

The most common method of making flutter measurements on rotating turbomachinery is with blade-mounted strain gages. However, recently developed techniques using digital data analysis of signals from stationary high-response pressure transducers have been used to determine the characteristics of flutter. Application of these techniques could greatly reduce reliance on strain gages and the required signal transmission hardware.

Case-mounted, high-response pressure transducers are aligned in the direction of the rotor chord from the leading edge to the trailing edge of the rotating stage. Additional transducers are located in the engine case at the midchord positions. The data from these measurements are recorded on a multichannel frequency-modulated magnetic tape recorder. The data are analyzed with digital spectral analysis procedures using the fast Fourier transform algorithm. These procedures allow construction of the rotor vibratory patterns during flutter. In addition, the flutter frequency can be accurately determined from measurements from two transducers at different circumferential locations.

The analysis of pressure transducer signals during flutter has the advantage over strain gages of allowing identification of complex vibratory patterns. Since the flutter is observed from a stationary reference frame, the spectral analysis decomposes the flutter into its constituent waves that show up as shifts from the true flutter frequency. This decomposition of a flutter mode is desirable because it facilitates comparison of experimental results with theoretical stability analyses that are performed in terms of a single flutter wave. To accomplish this with strain gages would be very costly since virtually every blade would have to be instrumented.

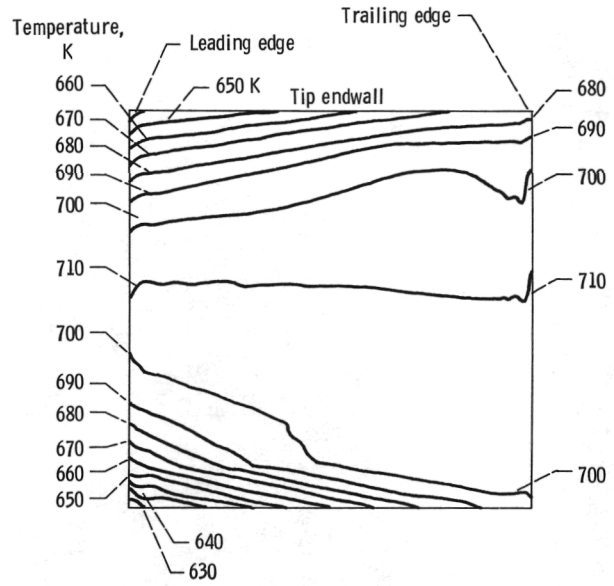

Prediction of turbine inlet temperature profile distortion on stator vane pressure surface

These spectral analysis techniques for determining flutter characteristics have also been extended so that pressure transducer data can be used for on-line flutter monitoring. This will enhance the identification of instabilities and supplement present monitoring schemes.

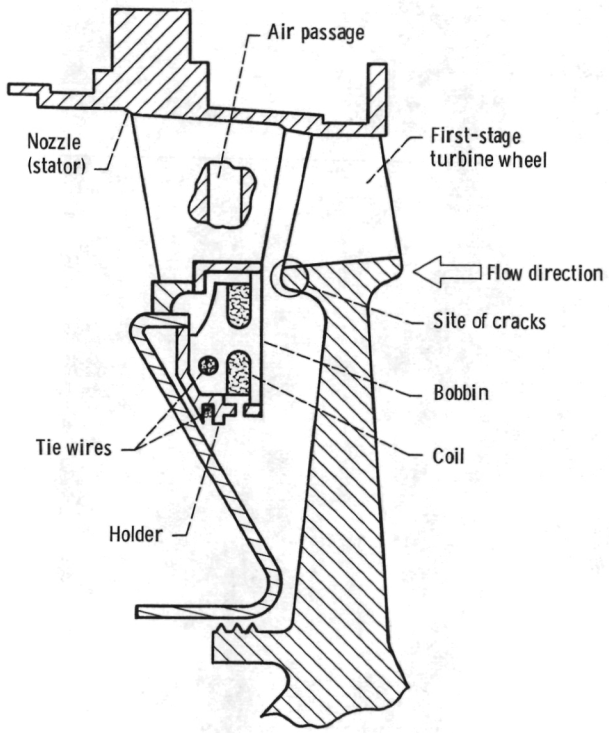

Turbine disk crack detector installed

Application of a Flight-Line Turbine Disk Crack Detector to a Small Engine

A turbine disk crack detector has been developed that is intended for use as a flight-line crack monitor. The system consists of an eddy current sensor and its cables within the engine, external connecting cables, and a remotely located electrical bridge and signal analyzer. As the turbine spins, the rotor is monitored by the sensor for radial surface cracks emanating from the interblade region of the rotor. Because the bridge is self-balancing, it automatically adjusts to changes in average coil inductance and resistance caused by temperature effects and variations in disk-to-sensor spacing.

The sensor is a coil of insulated wire wound on a ceramic bobbin mounted in the nozzle. It is located approximately 2½ mm (3/32 in.) away from the face of the downstream side of the first-stage turbine disk, where experience has shown that cracks are likely to occur. The coil leads pass through cored nozzle vanes and are joined to the sensor cables. The coil and coil leads are cooled by air through the core passage in the vanes.

A test cell at Lewis was prepared for evaluating the system on a small military engine. A disk with service-induced cracks was installed in the test engine. With the engine operating at ground idle conditions, the system was able to detect a crack 3 mm (1/8 in.) long. This is considerably shorter than the critical crack length. The sensor was subjected to all normal engine operating regimes. The coil withstood over 25 hr of operating time and over 35 starts and stops without failure.

Thermoelectric Characteristics of Turbine Engine Alloys

Part of the work to improve the durability of the hot sections of turbine engines is the development of sensors to measure the heat flux imposed on combustor liners, turbine blades, and vanes. One design concept for heat flux sensors is to measure the temperature difference across a section of the sensor through which the heat flux is transmitted by conduction. In this approach the engine part itself serves as a leg of the

thermocouple circuit. Therefore, it is necessary to determine the thermoelectric characteristics of turbine blade and vane materials.

A study of the thermoelectric characteristics of turbine engine alloys has been made. Thermoelectric data for more than 100 alloys were

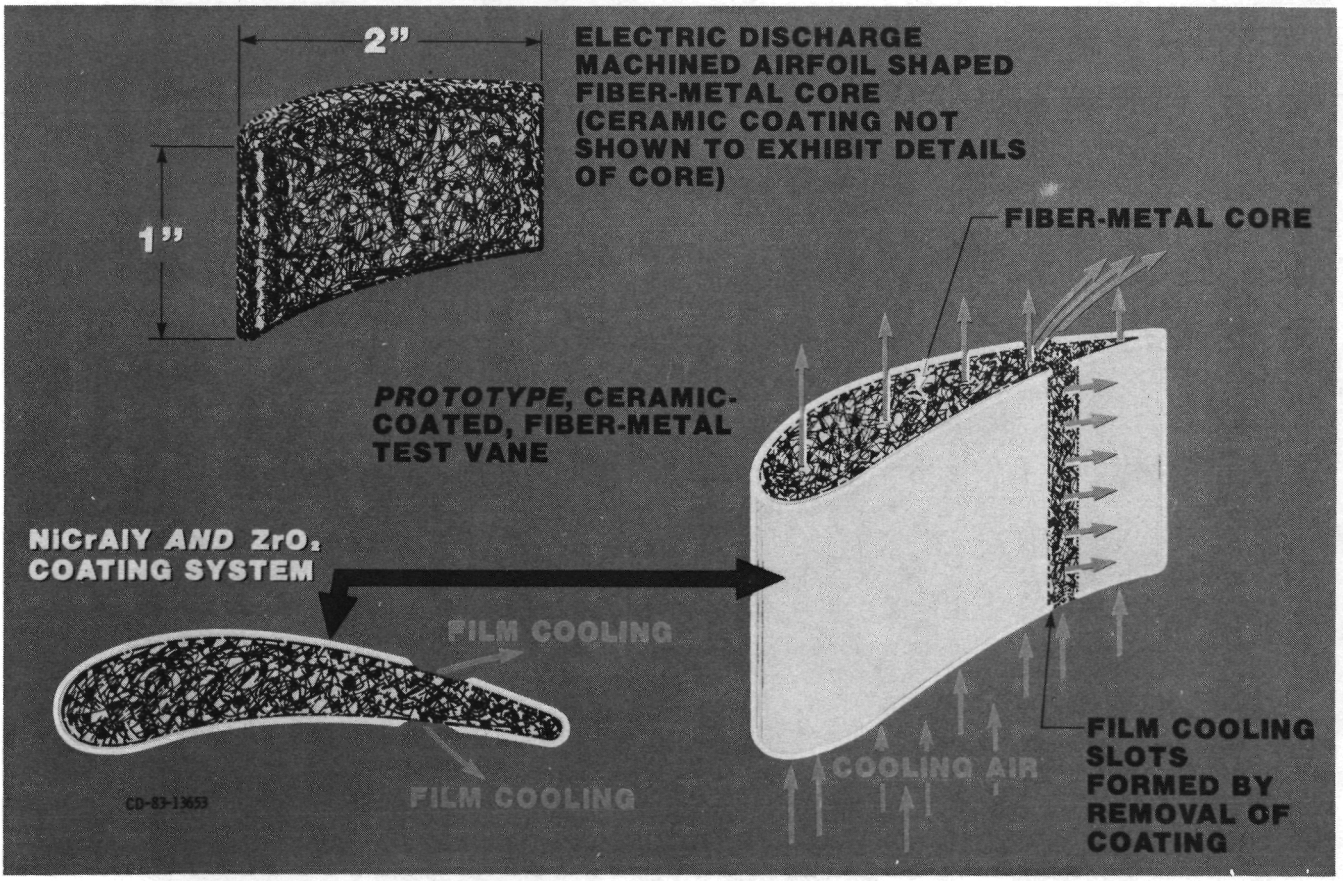

Ceramic-coated fiber-metal vane concept

studied. Data for some 35 previously uncalibrated alloys were included. The effect of alloy composition, internal structure, and physical properties on the level and stability of thermoelectric potential was determined. The allowable maximum usage temperature of a turbine blade or vane alloy as a thermocouple was defined. Heat flux sensors using this design

concept have been made for combustor liners and have been used in combustor liner tests at Lewis. Sensors are now being built into turbine blades and vanes.

Ceramic-Coated Fiber-Metal Airfoil Cooling Concept

Turbine cooling concepts for gas turbine engines operating at high gas temperatures and pressures employ complex and expensive cooling schemes. An expendable and relatively inexpensive cooling concept using small amounts of cooling air would significantly lower the cost and improve the performance of future engines. Preliminary development efforts and heat transfer tests indicate that this cooling concept can be fabricated and that its cooling effectiveness compares favorably with conventional air-cooling concepts. Also, the tests have qualitatively substantiated theoretical predictions.

The basic vane concept consists of porous fiber-metal material shaped into an airfoil. The airfoil surface, but not the ends, is oversprayed and sealed with a zirconia ceramic coating. Cooling air, which convectively cools the porous fiber-metal core, may enter radially through either or both the top or bottom ends of the vane. The cooling air is discharged through film-cooling slots formed at the trailing-edge region of both the convex and concave surfaces. Tests show that the ceramic coating acts as an effective thermal barrier (i.e., heat insulator) and that the fiber-metal material allows a thicker ceramic coating than possible with solid-metal air-cooled vane shells. Also, the fiber-metal core simultaneously provides an effective aerodynamic load-carrying capability and a good internal cooling configuration. However, there are problems that remain before the understanding of cooling phenomena in fiber-metal materials can be successfully applied to engineering design. Under a grant from Lewis, the Department of Mechanical and Aerospace Engineering at Case Western Reserve University has been providing much needed data and mathematical models for better prediction of convection cooling heat transfer characteristics of air flowing through porous, fiber-metal materials.

Advanced Turboprop Technology

Advanced turboprop propulsion systems have the potential for achieving large fuel savings (15 to 20 percent) on future aircraft with high subsonic cruise speeds. Engine studies recently completed by the three large aircraft engine manufacturers have indicated that the optimum engine cycle would have an overall pressure ratio of 35 to 40 and a turbine inlet temperature of about 2500° F at takeoff. Engine configurations were evaluated on the basis of mechanical design, performance, reliability, maintenance, and environmental considerations. Two- and three-spool engines with axial and axial-centrifugal compressors were predicted to have the lowest fuel and direct operating costs.

Designing the advanced turboprops for such a propulsion system is a challenging task that requires advanced computer analysis techniques. The preliminary design of a 9-foot-diameter advanced propeller with eight blades was completed. The latest state-of-the-art computer analysis and iterative design procedures available were used to determine the structural,

aeroelastic, and stability characteristics of the blades. These design tools were developed jointly by personnel of the Lewis Research Center and the contractor, Hamilton Standard. Numerous aerodynamic and structural configurations of the blade were analyzed before a suitable blade configuration was obtained.

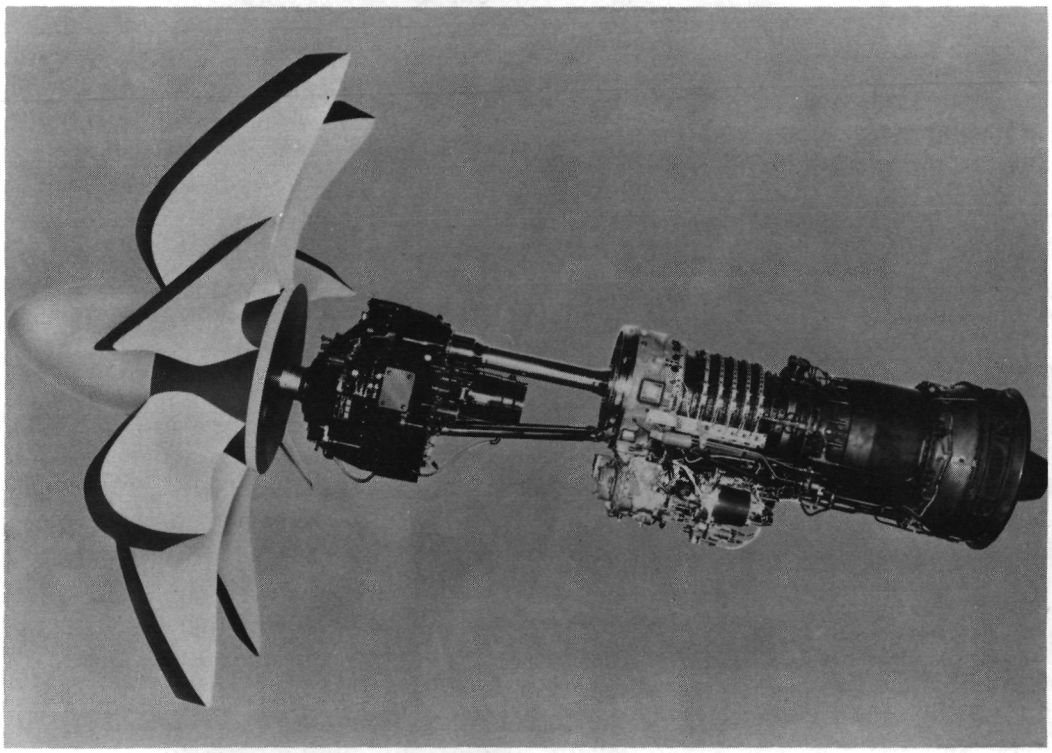

Mockup of proposed 9-foot-diameter advanced turboprop propulsion system

Analysis of Installation Effects on Turboprop Noise

A drawback to use of the turboprop as an efficient means of aircraft propulsion is the fact that it may produce considerable noise, particularly within the cabin, but also in the community. This has spurred research into turboprop noise sources. When the turboprop is operating in a uniform axial flow, noise is associated with forces on blades and flow disturbances that are steady in the blade frame of

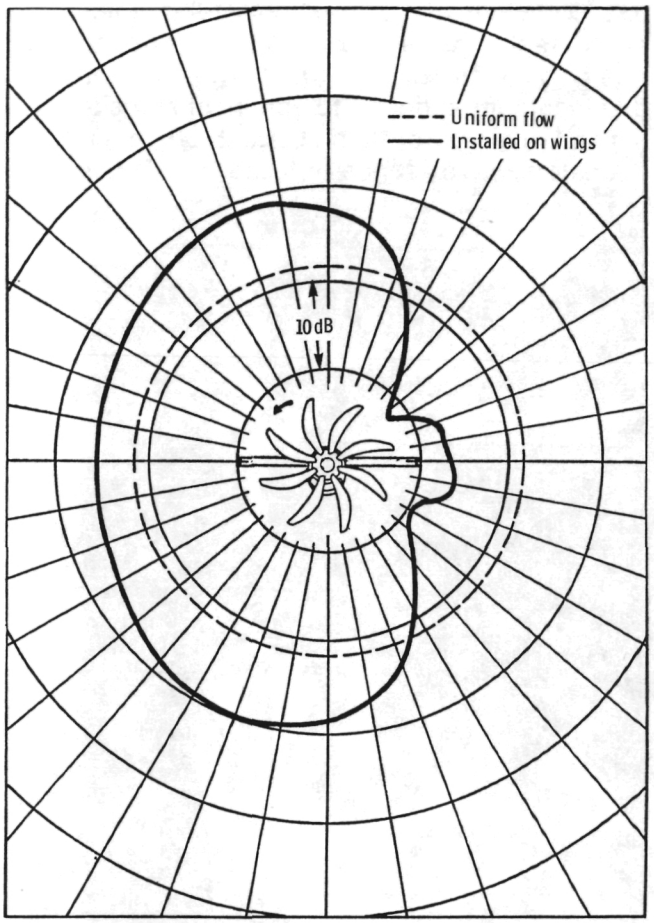

Directivity of fundamental tone in plane of propeller

reference. However, when it is installed on a wing, the propeller will operate at an angle to its inflow, which is also spatially nonuniform, because of the mean flow around the wing and engine nacelle. This flow nonuniformity produces unsteady blade forces, which contribute to the noise field. Preliminary experimental investigation of installation effects shows that substantial noise can result.

The relative importance of unsteady noise sources is determined both by the unsteady aerodynamic response of the propeller blades and by the efficiency with which the resulting unsteady blade forces radiate acoustic disturbances. The purpose of this analysis was to estimate the effect of inflow angle and wind-induced installation effects on turboprop noise. The unsteady noise source was found to be comparable to, and sometimes significantly larger than, the steady source. In addition, the directivity of the installed propeller was predicted to be asymmetric about the propeller axis, in contrast to the uniform directivity in uniform flow. The increase in noise on one side of the propeller and decrease on the other can be used to advantage. By choosing the proper direction of propeller rotation with respect to the wing and cabin (up and inboard), the noise reaching the cabin can be reduced. The approximate analysis provides guidelines for more elaborate theoretical and experimental investigations.

In-flight Measurement of Far-Field Turboprop Noise

Achieving acceptable noise levels is a key objective of research aimed at realizing the potentially large fuel savings associated with advanced, high-speed turboprop propulsion systems. Cabin noise, which depends on noise levels close to the propeller (the near field), is the subject of much analytical and experimental work. Community noise, which depends on the propagation of the noise to large distances (the far field), has received much less attention. The propeller blade tips move at supersonic speeds

that create shock waves on the blades. One of the unanswered community noise questions was whether these shock waves could propagate to the ground during aircraft cruise to create a special community noise problem. Since no ground-based facilities exist in which far-field noise can be measured at cruise conditions, a formation flight technique was employed.

A Learjet measurement aircraft with microphones in the nose and wing tip was flown in formation with the Jetstar test bed aircraft, which had a model high-speed propeller mounted atop the fuselage. Propeller tone noise levels were measured over a range of aircraft separation distances and fore and aft angles during formation flights at cruise speeds (Mach 0.7 to 0.8). Distances and angles were determined by photographs of the Jetstar from the Learjet. The rate of decrease of the propeller tone levels with distance corresponded to spherical spreading at separations greater than about 25 propeller diameters. No evidence of lesser falloff rates

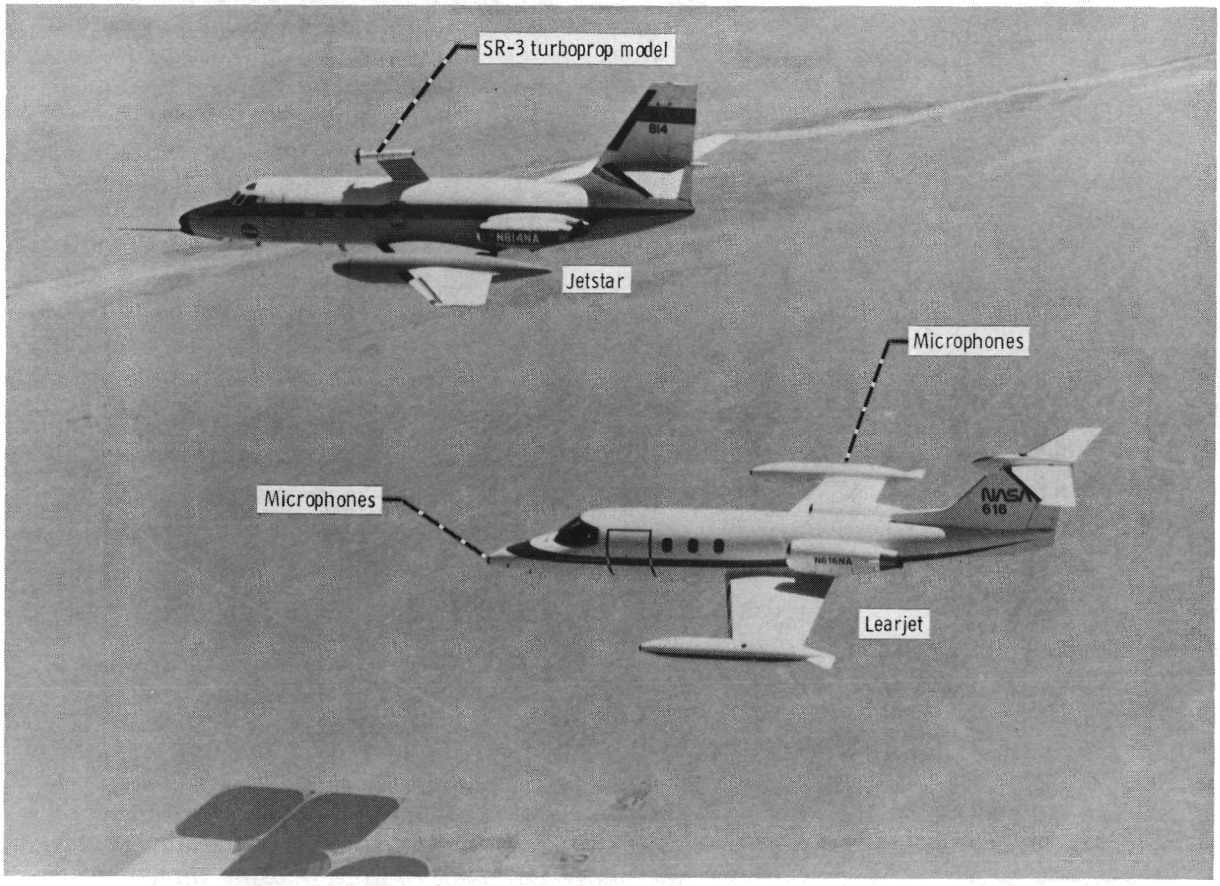

Jetstar and Learjet in flight

indicative of shock-wave propagation was found at large distances. Extrapolation of sound levels from cruise altitude to community areas based on these results indicate that community annoyance due to high-speed propellers on en route aircraft is unlikely.

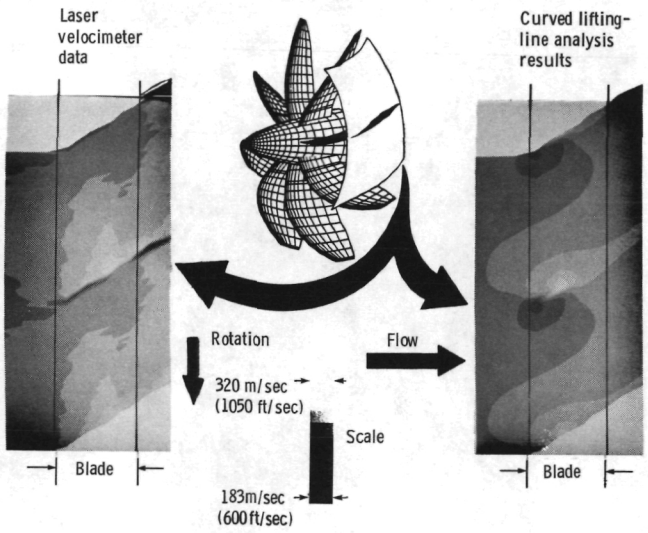

Comparison of LV data and curved lifting-line predictions for SR-3 propeller at Mach 0.8

Enhanced Prediction and Measurement of Propeller Flow Fields

Advanced turboprop propulsion offers the potential for large fuel and operating cost savings for future aircraft operating at high subsonic flight speeds. To achieve these benefits, new and complex analytical prediction techniques are being developed as part of the NASA Advanced Turboprop Program. Experimental data have been used to evaluate and verify these advanced analysis methods.

An argon ion laser velocimeter (LV) has been used in the Lewis 8- by 6-Foot Wind Tunnel to measure the flow field around an advanced eight-blade propeller with 45° tip sweep. The resulting data represent the first complete flow survey of an advanced propeller operating with transonic flow velocities. The laser velocimeter data have been compared with results from a new curved lifting-line analysis. The analysis includes the effect of blade sweep and has a better wake model than classical propeller analysis methods. Comparing the nonintrusive LV measurements of velocity with the analytical predictions shows good qualitative agreement. The comparisons are enhancing the understanding of blade loading, shock wave configuration, tip vortex development, and viscous wake effects in these high-speed propellers.

Energy Efficient Engine

The Energy Efficient Engine Program, which was started in January 1978, is now virtually completed with the full operational testing of the General Electric experimental turbofan engine. This engine, which incorporates the new technologies from the component efforts, completed 65 hr of sea-level static performance evaluations. Results of the test indicate that a specific fuel consumption reduction of 13.2 percent would be achieved at the cruise condition with this one-of-a-kind research engine. This is in comparison with the reference CF6-50C engine. Excellent operating characteristics and efficiencies were demonstrated over a wide range of power settings, including startup, for this high-pressure-ratio engine. All goals for the experimental engine were met. Also during the year, an advanced benefit-cost study was completed at Pratt & Whitney that identified efficiency gains beyond the energy efficient engine and established a technology plan for achieving them. From the results additional fuel

savings up to 24 percent over the energy efficient engine can be projected for turbofan engines in the year 2000 and beyond. Technology derived from the Energy Efficient Engine Program has been applied to CF6-80C, PW2037, and PW4000 engines.

Use of Electron Spin Resonance to Study Fuel Thermal Stability

Aviation turbine fuels with broadened properties or non-petroleum-derived fuels may have low thermal stability because of their high aromatic and heteroatom content. Deposits that result from the degradation of these fuels can have detrimental effects on aircraft fuel systems. The chemistry of fuel degradation involves primarily free radical reactions.

With support from Lewis, electron spin resonance (ESR) equipment has been developed and used to study the formation and reactions of short-lived free radicals in hydrocarbons at high pressures and temperatures. With this technique, free radicals can be produced in fuels either photolytically or thermally. The stressed fuels can be recycled or diverted to a gas chromatograph for product analysis. This permits determination of the mechanisms and kinetics of the reactions involved. In the flow system used in conjunction with the ESR spectrometer a liquid sample contained in a reservoir is purged with helium to remove dissolved oxygen. The liquid flows to a high-pressure pump, through a silica capillary that traverses the microwave cavity of the ESR spectrometer, and then to a backpressure regulator that controls the system pressure. The liquid exiting the regulator is at atmospheric pressure and can be recirculated or collected without recirculation for product analysis.

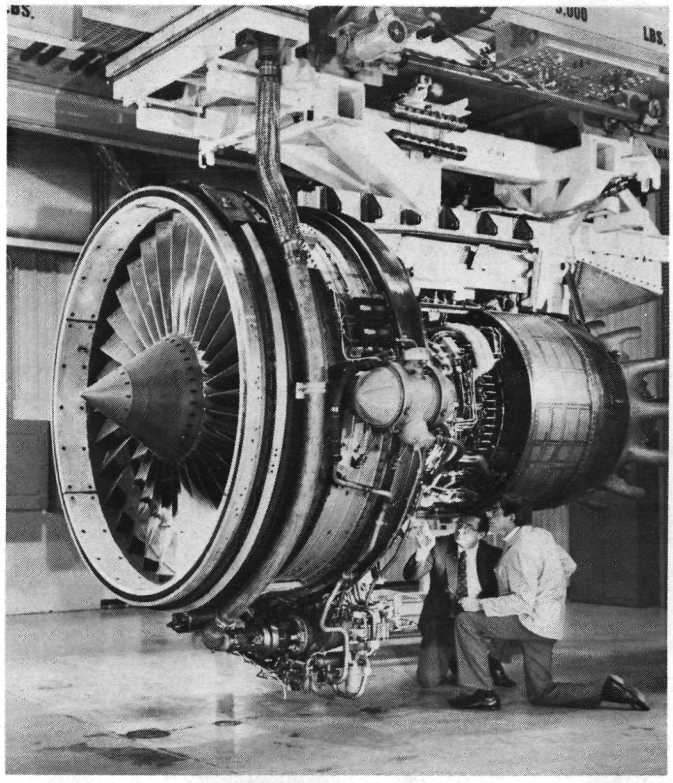

NASA-GE energy efficient engine

Regenerative, Intercooled Turbine Engine

Rising fuel costs and international competition in the area of general aviation have given rise to increased interest in small-engine fuel efficiency.

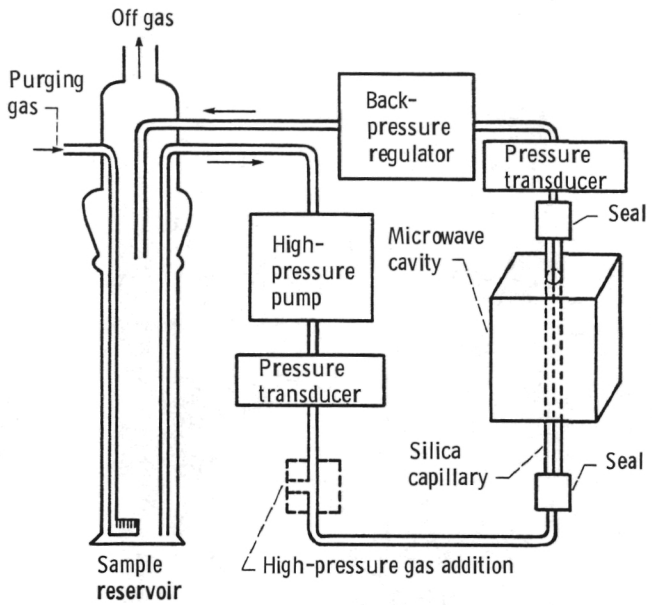

Flow system for fuel thermal stability studies using electron spin resonance spectrometer

One approach to overcoming the adverse effect of small size on the performance of this class of engine is to incorporate a regenerator and an intercooler. A regenerator is added aft of the last turbine to extract some of the heat in the gas before it is exhausted. This heat is then returned to the cycle. Intercoolers lower the compression work for a given overall cycle pressure ratio. Contracted and in-house studies indicate that a regenerative intercooled turbine engine (RITE) uses 50 percent less fuel than a current turboshaft engine. Because the RITE for aircraft application would make use of the technology developed for automobiles in the Advanced Gas Turbine (AGT) Program, under DOE and NASA sponsorship, costs associated with the heat exchangers may not be prohibitive. The RITE may have application for general aviation and commuter aircraft, auxiliary power units for commercial aircraft, and ground power.

Turbine Engine Contingency Power

Currently, in order to satisfy one-engine-inoperative requirements, twin-engine helicopters are designed with oversized engines. It has been recognized that payload or mission capability could be significantly increased by reducing fuel consumption with smaller, lighter engines that have a contingency power capability. At present a cooperative Army-NASA program at Lewis is focused on demonstrating the feasibility of one contingency power concept—water addition to the turbine cooling air to maintain acceptable turbine blade metal temperatures during augmented combustor burning. Tests of a T700 turboshaft engine employing this approach are scheduled in fiscal year 1985 at Lewis. Concurrently, under Lewis direction the General Electric Company, with support from Sikorsky Aircraft is analyzing the merits of several promising power augmentation concepts. This NASA-sponsored effort is aimed at quantifying actual benefits from using engines with contingency power systems in both military and civil rotorcraft and identifying areas where technology improvements are needed. The interim study results appear promising and areas of opportunity for future research focused on turbine power augmentation are being identified.

Transient Heat Conduction Analysis of Electrothermal Deicers

The formation of ice on aircraft components can seriously affect aircraft performance since it greatly increases drag and decreases lift. Thus, future advanced aircraft must have equipment for ice removal or prevention that is lightweight and reliable with low power consumption. Electrothermal deicing systems operate on the principle of cyclic heating of discrete elements of an aircraft's surface to periodically remove the ice that forms there. The energy requirements are significantly less for deicing systems than for anti-icing systems, which prevent any ice formation on the protected surfaces.

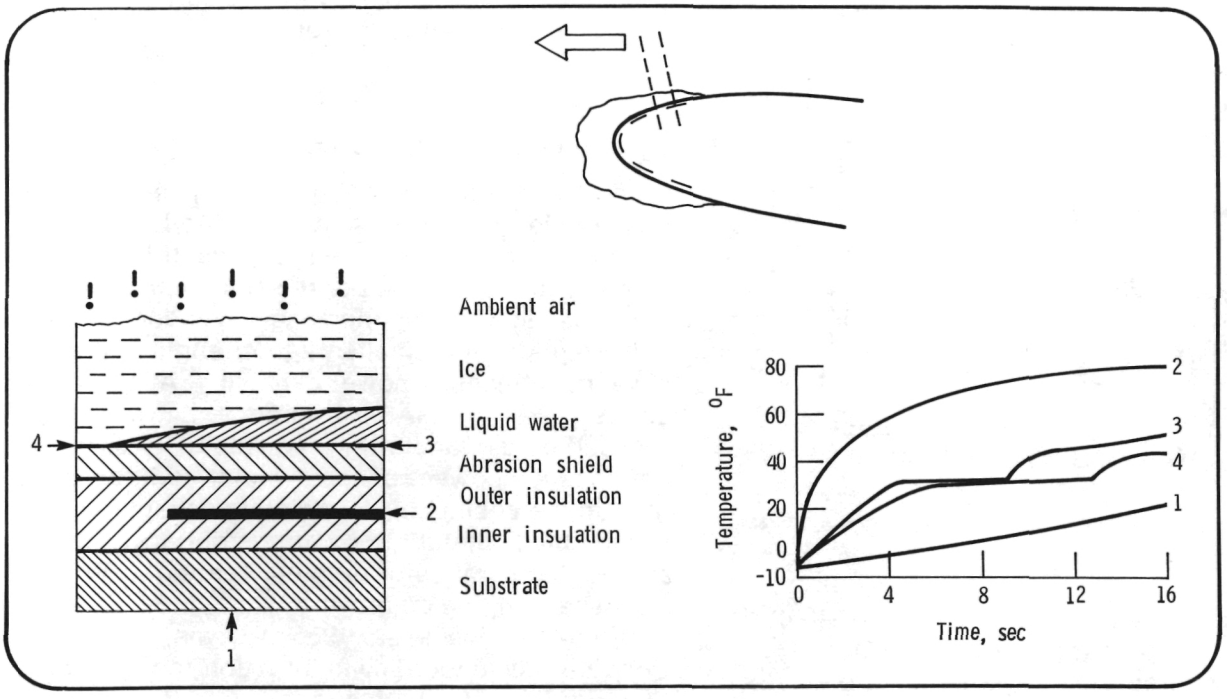

Two-dimensional transient heat conduction analysis of electrothermal deicers

As part of NASA's rotorcraft and aircraft safety programs, a new computer analysis code was developed by the University of Toledo that predicts the transient performance of electrothermal deicers. The code solves the finite-difference, transient heat conduction equations in two dimensions for typical electrothermal deicer configurations. This code is applicable to electrothermal deicer systems being developed by many helicopter companies for rotor blade deicing. The code is unique in that it can analyze the moving water-ice interface that can occur with thermal deicers.

Rainbow Schlieren for Flow Visualization

The schlieren optical technique used to observe nonuniformities in transparent media, especially fluid flows, has been enhanced in a new system that features visualization in all colors of the visible spectrum. The schlieren method involves selective filtering of white light that has traversed a nonuniform medium and has been refracted by the nonuniformities. In a new version of the apparatus the usual knife-edge filter has been replaced by a transparent rainbow bull's-eye filter with a clear center. With this filter nonuniformities appear colored against an otherwise white background. Observed colors are associated with measurable refraction of the light, which, in turn, can be used to evaluate refractive index, temperature, or density changes in the medium. This has been done in a number

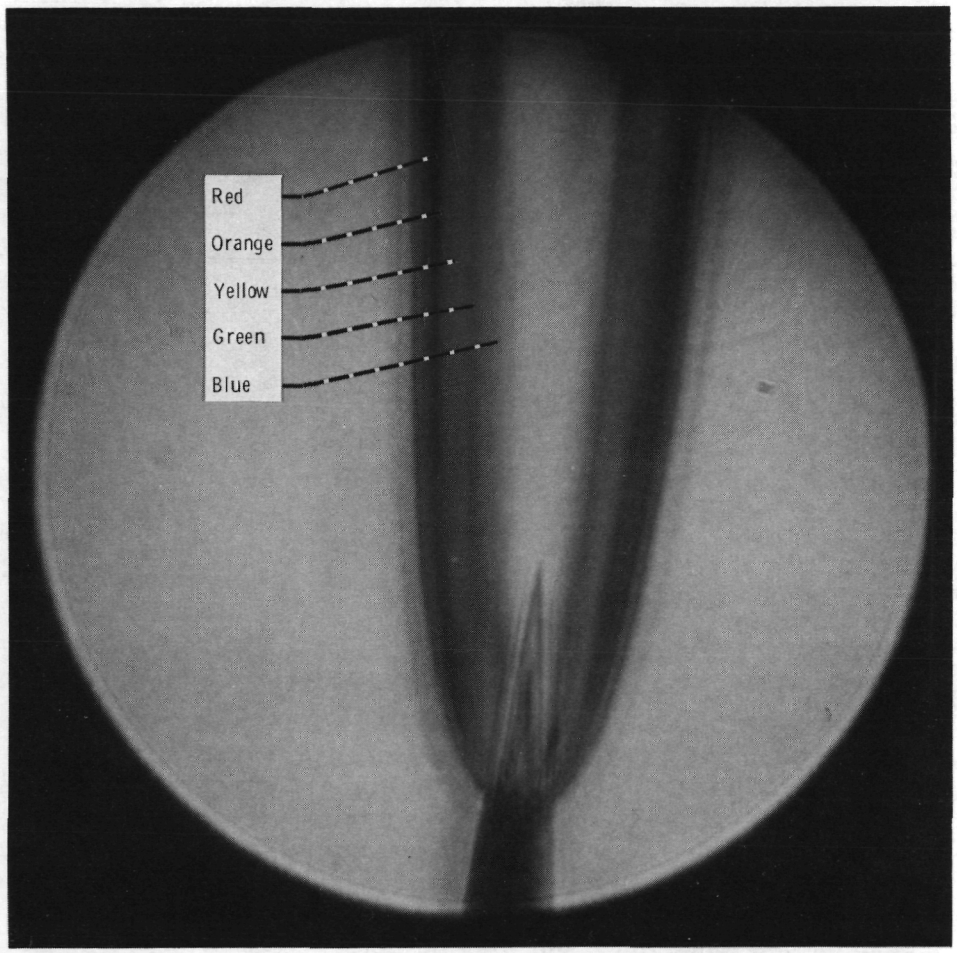

Rainbow schlieren of acetylene flame

of laboratory experiments. In addition, the rainbow schlieren is being used to evaluate flows in a two-dimensional flutter cascade. Rainbow recordings are also being made at the 10- by 10-Foot Supersonic Wind Tunnel.

Window Aberration Correction using Holographic Optical Elements

Multifaceted holographic optical elements were used to correct aberrations introduced into an optical measurement system by a curved window. This element was developed by Lewis personnel in conjunction with Spectral Science of Minneapolis, Minnesota. This element could be used, for example, in both the focusing and receiving optics of a laser velocimetry system. For this experiment three green beams and two blue beams in a horizontal plane were brought into coincident focus inside a thick-walled transparent cylinder. The ability to focus these beams and to correct the aberration caused by the cylinder was built into the holographic elements for representative locations within the cylinder. The principle is applicable for an arbitrary window geometry.

Design of Turning Vanes for Ames Wind Tunnel

A set of flow-turning vanes was designed for an Ames Research Center wind tunnel. The vanes are required to turn the flow 45° when the tunnel is operating using the 80- by 120-ft test section and to produce zero turning plus low loss when the 40- by 80-ft test section is being used. The original turning vanes were built with movable sections to direct the flow in the two modes.

The turning vane set was designed by using a combination of inverse design and flow analysis computer codes. A surface Mach number distribution that would produce low aerodynamic losses was specified for the 40- by 80-ft mode of tunnel operation. The inverse design computer code was used to calculate the vane shape that would produce the specified Mach number distribution. The performance of this vane geometry was then calculated for the 80- by 120-ft mode of tunnel operation by using inviscid flow analysis and boundary layer computer codes. Iterating between the inverse design and flow analysis codes led to a final blade shape that offers good performance in both modes of tunnel operation.

The performance of the vane set has been verified in 1/10th-scale wind tunnel tests conducted at Ames.

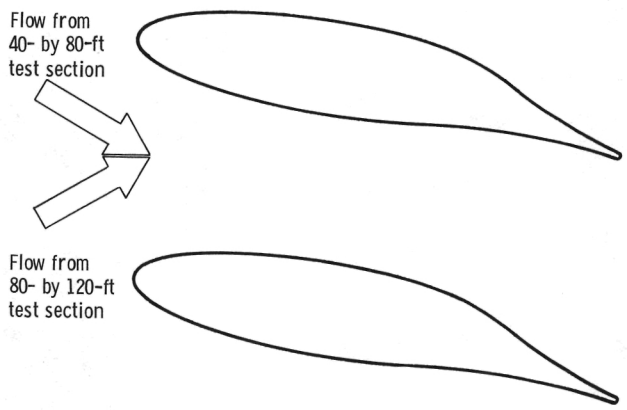

Turning vane set design

Title	Lewis contact	Phone number, (216) 433-4000, extension—	Headquarters program office
Highly Maneuverable Supersonic Inlets	Richard R. Burley	367	OAST
Three-Dimensional Viscous Marching Analysis for Supersonic Inlets	Thomas J. Benson	6130	OAST
Three-Dimensional Viscous Marching Analysis for Subsonic Internal Flow	Charles E. Towne	5520	OAST
Fundamental Flame Radiation Measurements	Francis M. Humenik Russell W. Claus	5211 6903	OAST
New Silicon Carbide Crystal Growth Process	J. Anthony Powell	353	OAST
High-Temperature Heat Flux Sensors	Howard F. Hobart	354	OAST
Dynamic Gas Temperature-Measuring System	Gustave C. Fralick	356	OAST
Computer Code for Dilution Zone Mixing	James D. Holdeman	5306	OAST
Prediction of Turbine Inlet Temperature Profile Distortion	John R. Schwab	6104	OAST
Flutter Characteristics from Stationary Pressure Transducers	Anatole P. Kurkov	5242	OAST
Application of a Flight-Line Turbine Disk Crack Detector to a Small Engine	John P. Barranger	354	OAST
Thermoelectric Characteristics of Turbine Engine Alloys	Raymond Holanda	356	OAST
Ceramic-Coated Fiber-Metal Airfoil Cooling Concept	Curt H. Liebert	5167	OAST
Advanced Turboprop Technology	Gilbert K. Sievers	317	OAST
Analysis of Installation Effects on Turboprop Noise	Paul A. Durbin John F. Groeneweg	5179 5372	OAST
In-Flight Measurement of Far-Field Turboprop Noise	Joseph R. Balombin John F. Groeneweg	5378 5372	OAST
Enhanced Prediction and Measurement of Propeller Flow Fields	Harvey E. Neumann	5272	OAST
Energy Efficient Engine	Carl E. Ciepluch	6644	OAST
Use of Electron Spin Resonance to Study Fuel Thermal Stability	Charles E. Baker	6696	OAST
Regenerative, Intercooled Turbine Engine	Gerald Knip, Jr.	223	OAST
Turbine Engine Contingency Power	Nick E. Samanich	5175	OAST
Rainbow Schlieren for Flow Visualization	Walton L. Howes	353	OAST
Window Aberration Correction Using Holographic Optical Elements	Harold J. Schock	5236	OAST
Design of Turning Vanes for Ames Wind Tunnel	Eric R. McFarland	488	OAST

Spaceflight

IR-100
High-Speed Switch Matrix for Advanced Communications Systems

Future geosynchronous communications satellites will provide coverage of the contiguous United States by employing many narrow spot beams to achieve high levels of frequency reuse. Such satellite systems will operate in a time-division multiple access (TDMA) mode and will require a switching network onboard the satellite to handle the routing between the multiple input-output ports. An onboard computer will control the switching system to assure the desired traffic routing connections.

General Electric and Ford Aerospace, under contract to Lewis, have each designed, fabricated, and tested switch matrix systems capable of handling 20 input ports and 20 output ports. Both designs use coupler crossbar architecture. Each of the 400 crosspoints consists of two stages of dual-gate gallium arsenide FET's operating in a switch amplifier mode. The crosspoints have demonstrated on-off-on switching speeds of less than 10 nsec. The 400 crosspoints can be reconfigured every 2 μsec and, through computer control, can consider a varying sequence of 500 000 input-output interconnections per second.

The crosspoint circuit was designed to operate at nominal frequencies of 4 to 7 GHz and was fabricated by using microstrip techniques. The circuit network has demonstrated useful bandwidths greater than 2 GHz.

Multiple-Beam Spacecraft Communications Antennas Using Monolithic Microwave Integrated Circuits

The monolithic microwave integrated circuit (MMIC) device offers the space communications antenna designer several advantages including increased functional capability for multiple fixed and scanning spot beams and potential savings in weight, size, and cost. Lewis is pursuing base R & T activities that will investigate and demonstrate the feasibility of such antennas and provide a data base supporting additional advanced development and ultimately application in future systems.

Two 1-yr configuration study contracts to identify and analyze promising dual-offset reflector configurations using 20-GHz transmitting MMIC modules have been completed by COMSAT and Harris Corporation. Both multiple fixed spot beam and multiple scanning beam concepts have been developed. A follow-on contract to design and fabricate an experimental antenna system for investigating these concepts will be awarded in late 1983. The experimental system, incorporating MMIC devices, will be tested at Lewis.

Lewis contracted with General Electric for a similar effort leading to a feasibility demonstration of 30-GHz receiving antennas that use MMIC devices.

Microwave Monolithic Integrated Circuit Development for Future Spaceborne Phased-Array Antennas

Implementing advanced communications satellite antenna systems requires the development of reliable, efficient, low-cost, solid-state microwave devices. Studies have indicated that systems using microwave monolithic integrated circuit (MMIC) devices offer substantial advantages over presently used devices and resulting system designs. An MMIC device provides an entire electronic function on a single semiconductor

chip without any external tuning. Lewis is pursuing the following MMIC developments, which promise maximum effect for future communications systems in the 30/20-GHz frequency range.

Lewis contracted with Texas Instruments to develop a monolithic variable-power amplifier module. The technology goals include an amplifier operating between 17.7 and 20.2 GHz with five-level digital output power control from zero to 500 mW. The power-added efficiency requirements range from 6 to 15 percent for output powers of 12.5 to 500 mW. In these programs submodules have been fabricated that demonstrate the various functions that will be

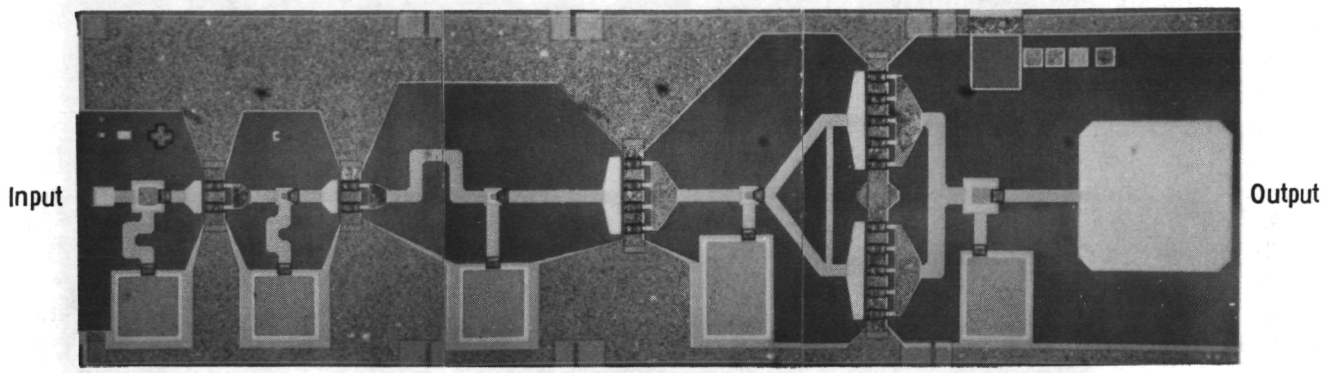

20-GHz four-stage monolithic amplifier (1.4 by 3.4 mm²)

Under a contract from Lewis, Rockwell is developing an MMIC transmit module. The technology goals for this contract include a power output of 200 mW at 15-percent efficiency, a gain of 16 dB, a five-step phase control from 0° to 180°, and a frequency band from 17.7 to 20.2 GHz.

necessary in the fully monolithic modules. Two parallel contracts to develop a 30-GHz monolithic receiving module were awarded to Hughes Electron Dynamics Division and Honeywell. Goals include a frequency range of 27.5 to 30 GHz, a noise level of 5 dB, a 4- to 8-GHz intermediate frequency, a radiofrequency-to-intermediate-frequency gain of 30 dB, and a five-level digital gain and phase control.

Tunneladder Traveling-Wave Tube

A tunneladder circuit for a high-power millimeter-wave traveling-wave tube (TWT), a concept that was evolved and analytically examined at Lewis, was successfully tested in two TWT's at Varian Associates. One of the TWT's is designed for operation as an uplink at 30 GHz; the other as a

40-GHz downlink space amplifier. The TWT's put out 400 W at saturation, have an instantaneous bandwidth of 600 MHz, and will be 50-percent efficient after augmentation with good multistage depressed collectors.

Long-Life Cathodes for Space Communication TWT's

An understanding of the mechanism of operation of impregnated cathodes employed in communications satellite TWT's is essential for improving reliability and attaining long life in such devices. Surface research has been conducted on cathodes at Lewis by means of Auger, X-ray photoelectron spectroscopy (XPS), and work function measurements. The results show that carbon and oxygen, which are normal impurities in the substrate tungsten used for impregnated cathodes, as minor surface constituents strongly influence electron emission from the cathode surface. Carbon as a surface contaminant is deleterious to electron emission, whereas low oxygen surface concentrations are advantageous. However, excessive oxygen on the tungsten surface also degenerates the electron emission capability of the cathode. These studies suggest that commercial impregnated cathodes can be improved by controlling the oxygen and carbon impurities in the tungsten matrix.

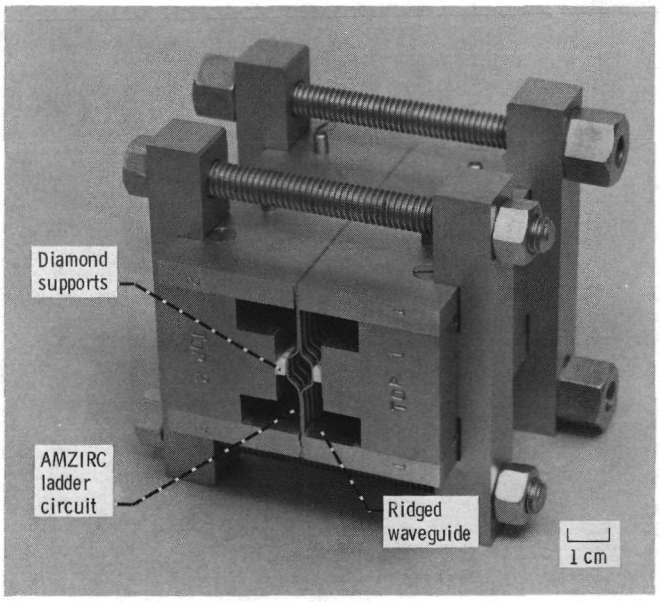

Varian tunneladder TWT cold test fixture

TWT Amplifier with Linear Power Transfer Characteristic and Increased Efficiency

A novel method to linearize the power-out versus power-in transfer characteristic of TWT's by internal modification of the phase velocity has been developed and evaluated on computers. (Actual verification in real TWT's is in progress but was not available at the date of this writing.) The phase velocity is being matched dynamically to the local condition of the beam with two major benefits:

(1) The power transfer characteristic approaches that of a hard limiter

(2) The interaction efficiency is increased by 1 to 2 dB

If successful in verifications the dynamic velocity taper will have a significant effect on space communications satellites.

Baseband Processor Unit for Advanced Communications Satellites

The next generation of communications satellites may use a baseband processor (BBP) to provide message-routing capability onboard the satellite.

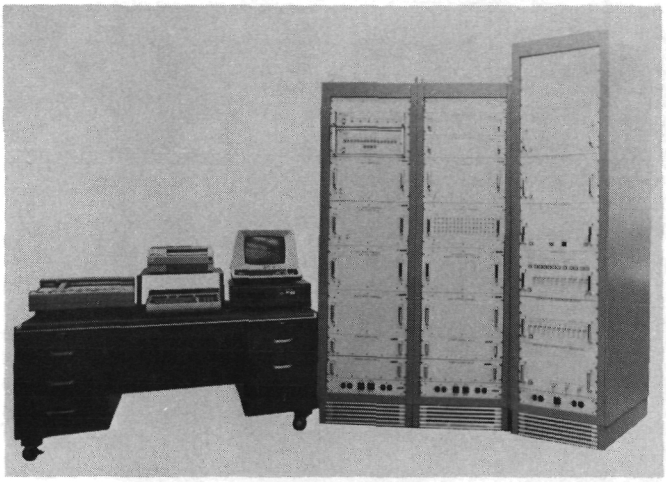

Baseband processor and special test equipment

The BBP is intended for use in switching messages among a network of 2000 or more small Earth terminals served by the satellite. Uplink signals reaching the satellite consist of radiofrequency carriers modulated by digital data. The BBP fully demodulates and decodes the uplink signals and reduces them to their baseband content—digital data consisting of binary ones and zeros. These are stored in memory, switched digitally to the proper downlink channel, and then recoded and remodulated for transmission.

Motorola, Inc., under contract to Lewis, is developing the technology required to support detailed design and fabrication of a BBP for NASA's advanced communications technology satellite. Considerable progress has been made in developing both the architecture and technologically critical, custom large-scale integrated (LSI) circuits needed for a reliable, low-weight, efficient flight BBP. A proof-of-concept model using the critical LSI has been built and tested, and the basic operations performed by the BBP have been successfully demonstrated in the laboratory. Also, system software has been developed and tested and shown to provide correct control.

Title	Lewis contact	Phone number, (216) 433-4000, extension—	Headquarters program office
High-Speed Switch Matrix for Advanced Communications Systems	Ernie W. Spisz	713	OSSA
Multiple-Beam Spacecraft Communications Antennas Using Monolithic Microwave Integrated Circuits	Charles A. Raquet	475	OAST
Microwave Monolithic Circuit Development for Future Spaceborne Phased-Array Antennas	Godfrey Anzic	6197	OAST
Tunneladder Traveling-Wave Tube	Henry G. Kosmahl	6892	OAST
Long-Life Cathodes for Space Communications TWT's	Ralph Forman	6865	OAST
TWT Amplifier with Linear Power Transfer Characteristic and Increased Efficiency	Henry G. Kosmahl	6892	OAST
Baseband Processor Unit for Advanced Communications Satellites	Russell J. Jirberg	222	OSSA

Space Technology

Space Power

IR-100
High-Frequency, High-Power Capacitor

A 600-V, 125-A capacitor operating at 10 to 40 kHz was developed by Maxwell Laboratories under contract to Lewis during 1982. It received an IR-100 award as one of the 100 best new products of 1983 as determined by Industrial Research & Development magazine. To demonstrate the technology, a 0.83-μF capacitor was built that was 7 to 8 times smaller and lighter than a comparable commercial capacitor. This type of capacitor is essential to the development of lightweight and efficient large space power systems (25 to 100 kW). It is also expected to be used in ground-based power applications such as high-power, high-frequency power supplies, inductive heaters, and filter networks.

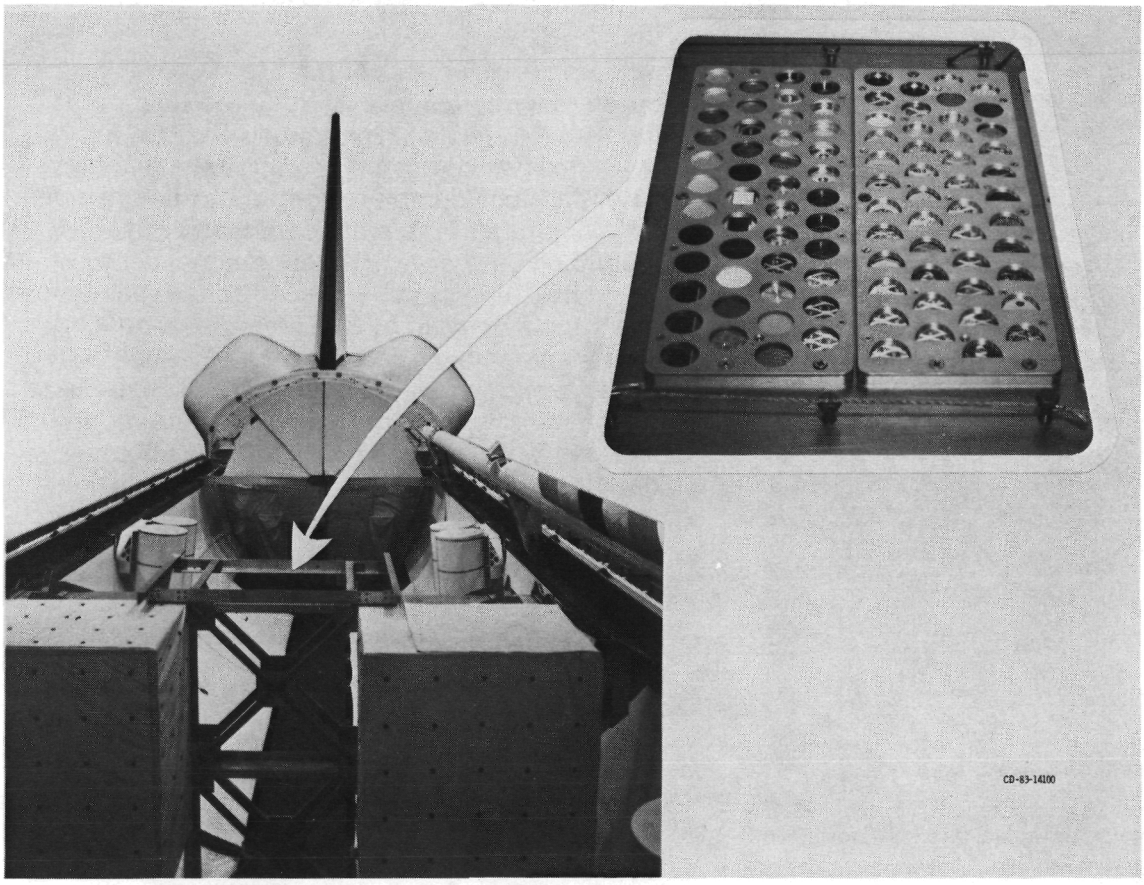

STS-8 atomic oxygen interaction experiment

High-Power, Fast-Switching Transistors and Diodes

High-power transistors and diodes have been developed for use in large space power system applications, such as a space station (25 to 100 kW), where both high voltage and high current capability are important to achieving minimum system mass. These devices can control voltages up to 1000 V and currents of 100 to 150 A, factors of 2 larger than for previously available devices. They also provide the fast switching times (0.5 μsec) and high power capability necessary for the development of the lightweight and efficient large space power systems of the future. Both the transistor and the diode will be commercially marketed because it is expected that they will provide substantial benefits in many terrestrial applications such as industrial robots and motor controls.

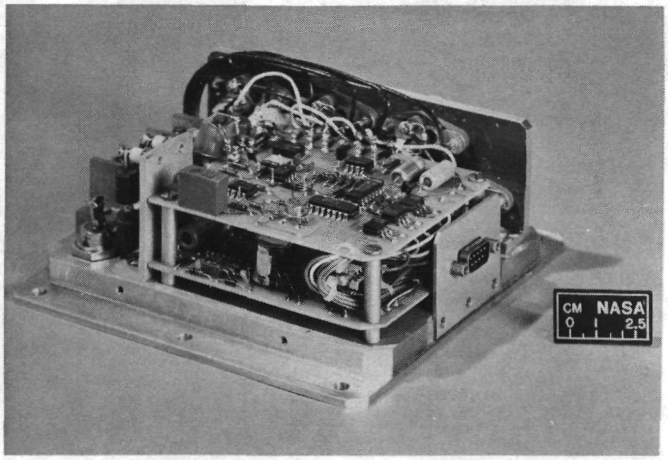

Remote power controller with metal oxide surface field effect transistors

Atomic Oxygen Interaction Studies

Shuttle flights 1 to 5 revealed that a wide variety of polymers and metals lose weight or change their optical properties as a result of exposure to the low Earth orbital environment. The postulated mechanism for this degradation, oxidation by atomic oxygen ions made energetic by the shuttle's orbital velocity, has been verified by simulations in Lewis vacuum facilities. Lewis is also investigating the synthesis of new materials suitable for protection of polymers. The materials, produced by ion beam sputter codeposition of metal oxides and polymers, have been found effective in protecting Kapton.

A variety of materials and coatings have been characterized for mass loss and optical degradation through both spaceflight tests and laboratory simulation of the low Earth orbital environment. The flight experiment, conducted on STS-8 from August 30 to September 5, 1983, characterized the degradation of current materials and Lewis-developed protective coating materials. By providing a comparison with the Lewis laboratory tests, these flight tests increase our confidence in laboratory testing and thus provide the ability to develop durable spacecraft materials without testing in low Earth orbit.

High-Voltage, High-Power Remote Power Controllers

There is a recognized need for remote power controllers (RPC's) that can switch multi-hundred-kilowatt loads and interrupt overloads very rapidly to protect the many semiconductor devices in space power systems. Circuit designs were developed at Lewis for two general types of RPC's. The designs all combine remote switching and circuit breaker functions with very fast overload protection. Power-switching devices used in these designs are the relatively new gate-turnoff thyristor (GTO) and power metal oxide surface field effect transistor (MOSFET). With appropriate switching devices and minor modifications, these circuits can be used to build RPC's covering a range of voltage and power levels limited only by the switching devices chosen.

The control circuit features a programmable overcurrent tripout that can be adjusted for both current level and time. For slight overloads, tripout typically takes several seconds. As the overload increases, the trip time decreases in a smooth curve until at fast trip (high overload) the RPC opens in 3 μsec. The devices have efficiencies close to 99 percent and are lightweight and small.

RPC's used on the shuttle have a voltage rating of 32 V at 20 A with a power loss of 2.5 percent. In contrast, the seven new RPC's (four with GTO's and three with power MOSFET's) have power capabilities to 52 kW, voltages to 1200 V, and power loss of less than 0.3 percent. These new RPC's could be an enabling factor for space station power systems.

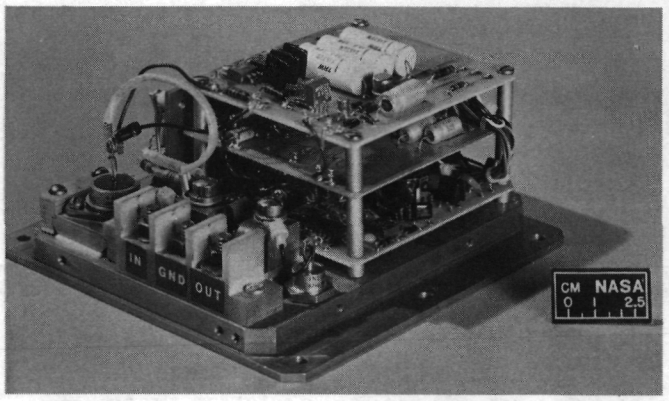

Remote power controller with gate-turnoff thyristors

Liquid Droplet Generator

Recent tests conducted at Lewis have demonstrated and confirmed controlled production of minute-droplet streams at vacuum conditions using 100-μm-diameter orifices (fabricated at Lewis) and a low-vapor-pressure, silicone-base fluid. A photographic method recorded droplet stream characteristics. This activity is part of a joint NASA–Air Force program on the liquid droplet radiator (LDR). The liquid droplet radiator is a new concept for heat rejection from spacecraft that offers large savings in mass and volume. Radiator concepts in use or in development use pumped-fluid and heat-pipe concepts. The heat transfer surface is metallic, the heat transfer fluid is confined in a sealed metallic enclosure, and surface coatings are needed to improve heat transfer efficiency. Armor or shielding is also necessary to minimize penetration by micrometeoroids and consequent loss of fluid. These systems neither store compactly nor are readily deployable. Problems of mass, stowage, and assembly in space are associated with these radiator designs.

In the LDR concept the heat transfer fluid is ejected into space as directed streams of minute

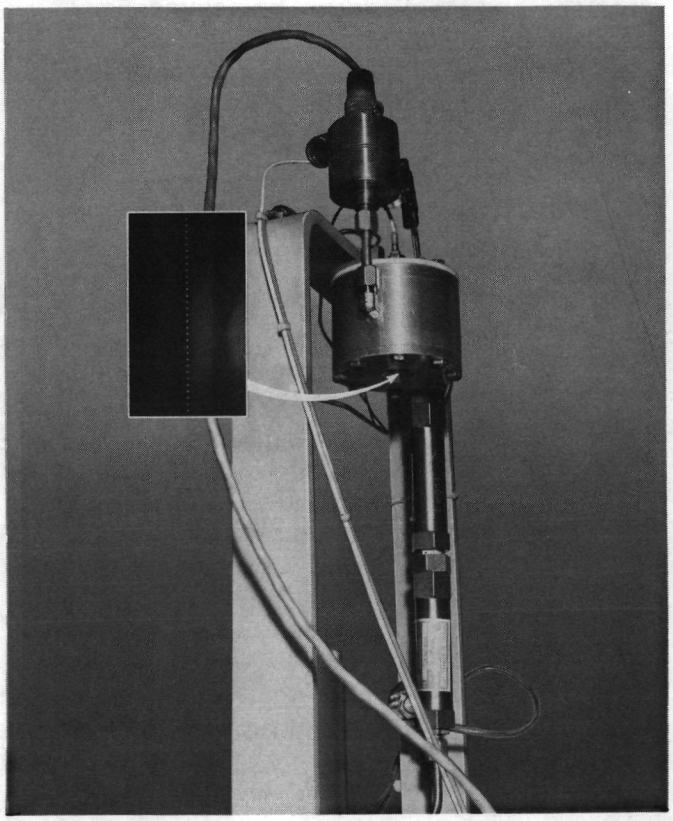

Liquid droplet generator

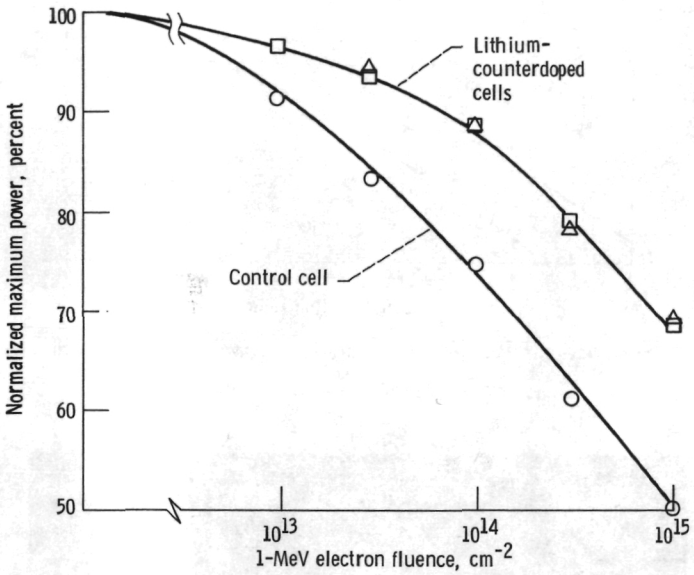

Performance of lithium-counterdoped solar cells

droplets. Droplets cool by radiation to space as they travel to a collector in flight. They are gathered and recycled within the spacecraft. This concept eliminates the need for micrometeoroid protection, surface coatings, and assembly in space. Key problems are generation of accurate droplet streams, collection of all droplet streams, and low-vapor working fluid properties. The recent results will be used in furthering experimental studies to investigate heat transfer and stream trajectory characteristics, leading to a test radiator system design.

Lithium-Counterdoped Solar Cells

Future space missions will require increased end-of-life output power from solar cell arrays. To achieve this goal, researchers at Lewis have been seeking ways to minimize the degrading effects of space radiation on solar cells. One technique employed lies in adding lithium to the normally boron-doped base of silicon solar cells. This process, known as counterdoping, increases the radiation resistance of silicon solar cells. The results are shown in the accompanying graph, where the performance of a control cell without lithium is compared with the performance of lithium-counterdoped cells. Lithium counterdoping significantly increased resistance to the damaging effects of radiation. Continuing studies have identified the harmful defects and point the way toward obtaining even greater radiation resistance from lithium-counterdoped solar cells.

Miniature Gallium Arsenide Solar Cell

Two major objectives of the NASA program in photovoltaics are to reduce the cost and increase the lifetime of solar arrays used in space. These are particularly important concerns as satellite power requirements climb toward hundred kilowatt levels. One promising approach for achieving these objectives is to use concentrator arrays, rather than planar arrays. In the past, concentrator arrays were not considered for use because of their apparent high operating temperature. However, with a miniature Cassegrainian concentrator design operating at 125-suns geometric concentration ratio, a cell operating temperature of only 80° C was achieved. This compares favorably with the 55° C operating temperature of a planar array. The miniature size, reasonable operating temperature, and high concentration level are natural conditions for gallium arsenide solar cells.

Accordingly, Hughes Research Laboratory, under contract to Lewis, has produced a miniature gallium arsenide concentrator solar cell with an air-mass-zero conversion efficiency of 19 percent under the required conditions. Cell efficiency

increased with concentration level. The decrease in performance with increasing temperature was about half that expected for a comparable silicon solar cell. This cell is properly sized for assembly into the 5-cm-diameter miniature Cassegrainian concentrator element that forms the basic building block of the array. The small size of the cell (4 mm diam on a 5-mm-square substrate) substantially reduces the amount of active material in the array and should result in at least a threefold reduction in array cost. Future work will be directed toward further increases in cell efficiency and space qualification of cells and concentrator elements.

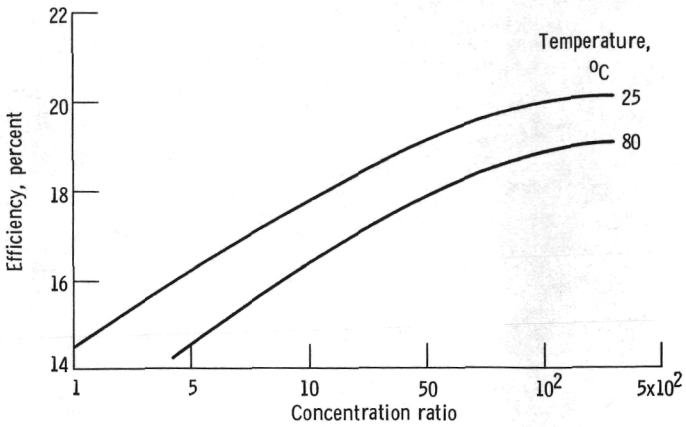

Performance of miniature gallium arsenide concentrator solar cell

New Design for Individual-Pressure-Vessel Nickel-Hydrogen Cell

Part of the Lewis nickel-hydrogen storage battery technology development effort is related to component improvements for the state-of-the-art individual-pressure-vessel (IPV) nickel-hydrogen cells that were developed for the Air Force. As a result of cell and component test programs carried out both in-house and under contract, several areas of deficiency were found in the current design for applications in low Earth orbit at deep depths of discharge. As a result of the continuing component improvement efforts related to the Lewis bipolar nickel-hydrogen concept, alternative materials suggested themselves for use in the IPV cells. Further, alternative ways of managing the oxygen recombination and endemic nickel electrode expansion phenomena became evident. All of these were combined into a modified design for this type of cell. A number of these cells will be life tested to validate the extended cycle life that is expected from these modified designs.

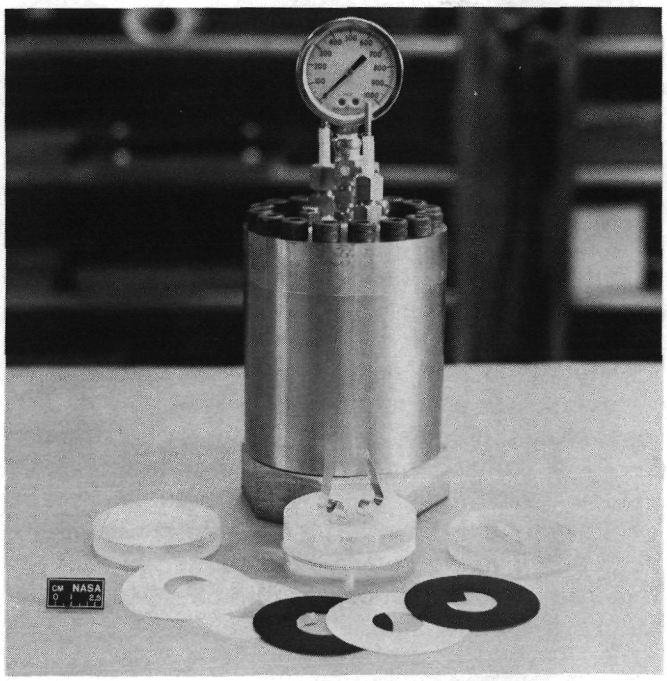

Boilerplate nickel-hydrogen cell (capacity, 1.5 to 6.0 Ah)

"Synthetic Battery Cycling Techniques" Film Supplement

A film supplement to NASA TM-82945, "Synthetic Battery Cycling Techniques," has been prepared. The film introduces the concepts of cell-to-cell

balance and other battery-related problems that need to be addressed when considering battery system design. The film, which for the most part has been taken directly from the screen of a color graphics stand-alone computer, covers a number of progressively more complex situations. The cell chemistries of the more advanced battery systems are quite different from those used in state-of-the-art systems. The film illustrates how these differences can affect the circuitry and design philosophy employed for these newer systems. The film is available through the NASA lending services under the name "Synthetic Battery Cycling Techniques" (C-310).

Scaled-Up Water Electrolysis Hardware

A very promising option for multikilowatt electrochemical storage systems makes use of fuel cells and water electrolyzers. State-of-the-art water electrolysis cells have an active area of 0.1 ft^2. Life tests on this size of cell have exceeded 20 000 hr with very little performance decay. This hardware would be too small for the storage system in a space station. Lightweight cells containing 10 times the active area have been designed, constructed, and successfully tested. Multicell stacks will be fabricated and life tested. This effort is part of an integrated program between Lewis and the Johnson Space Center that has as its objective the demonstration of breadboard versions of complete regenerative fuel cell systems.

Space Propulsion

Cryogenic, Long-Life Hybrid Bearings

The evolution of turbopumps over the last 10 to 15 years has placed significant new demands on bearing technology. Ball bearings used in current cryogenic turbopumps seriously limit life. To meet the needs of a fully reusable space transportation fleet, bearings are needed that have a minimum service life of 10 hr and 300 full transients. Another requirement is to provide increased damping to improve rotor stability.

A hybrid bearing, consisting of both rolling ball

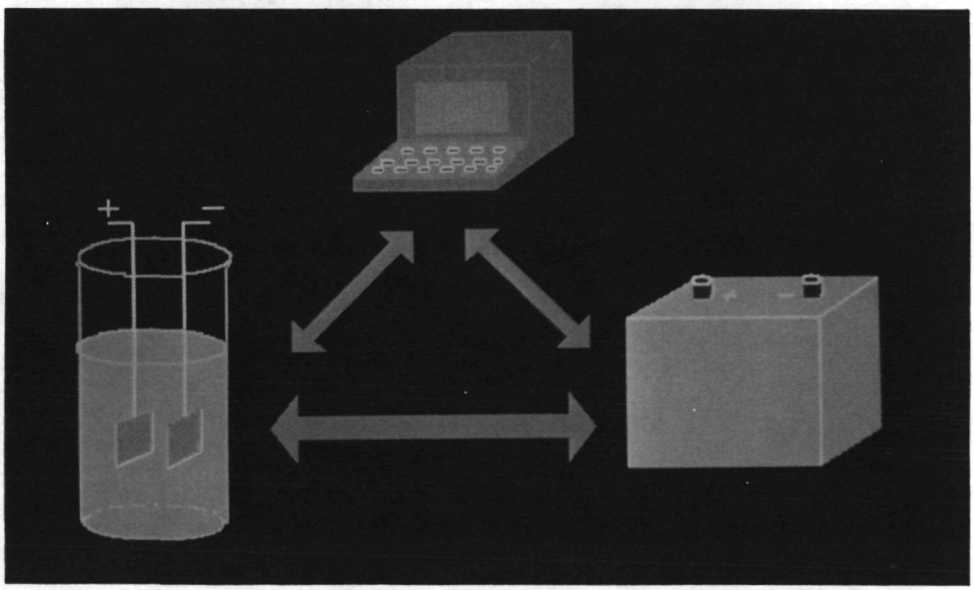

Frame from "Synthetic Battery Cycling Techniques" film supplement

elements and hydrostatic film elements, has been designed, tested, and shown to provide much longer life and improved rotordynamic characteristics. Two different experimental programs have been completed. A bearing tester was used to determine steady-state and transient operating characteristics and to conduct life tests. The tests were conducted in liquid hydrogen at speeds to 100 000 rpm and over a wide range of test conditions simulating those in an actual turbopump. A second test series was completed using an existing cryogenic turbopump that had been retrofitted with hybrid bearings. During these tests the feasibility of using the long-life bearings in an actual turbopump environment was successfully demonstrated.

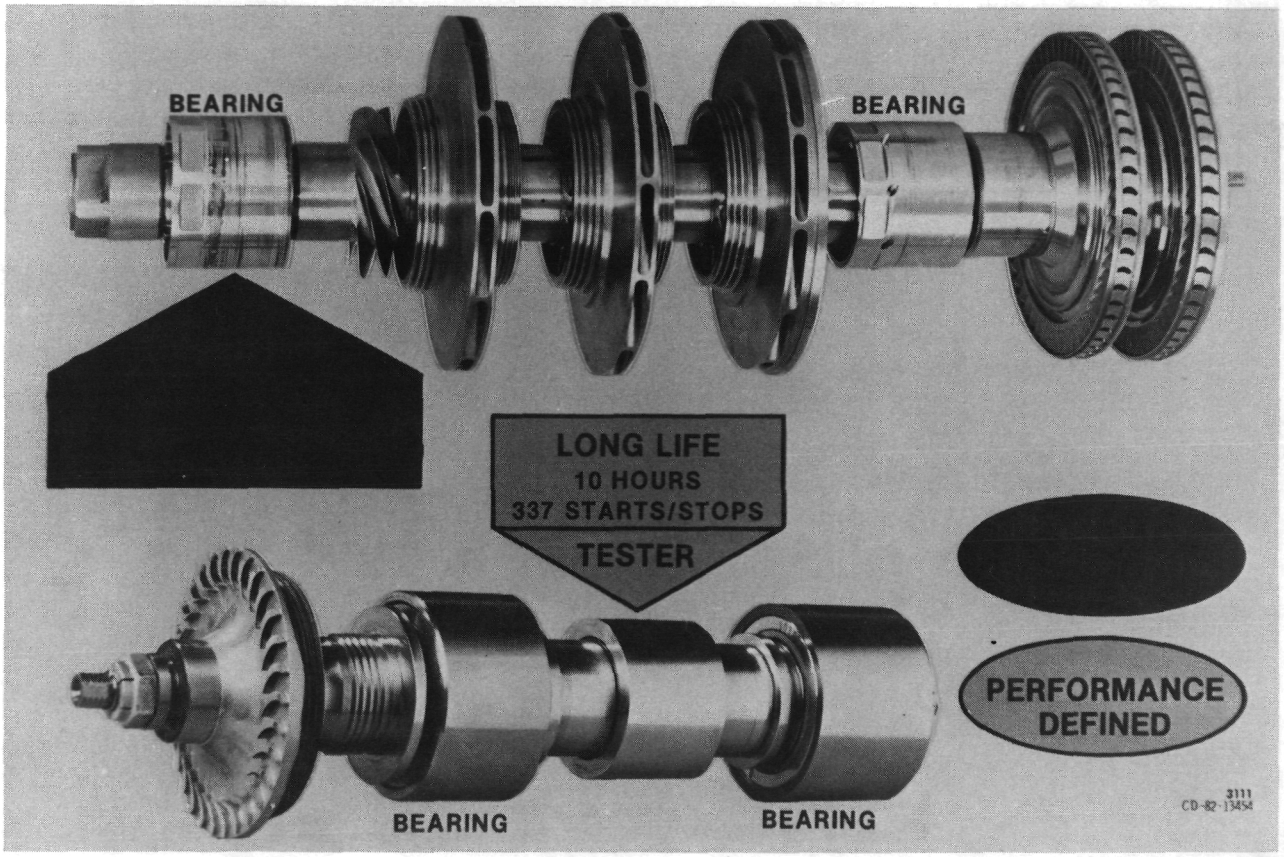

Cryogenic, long-life hybrid bearings

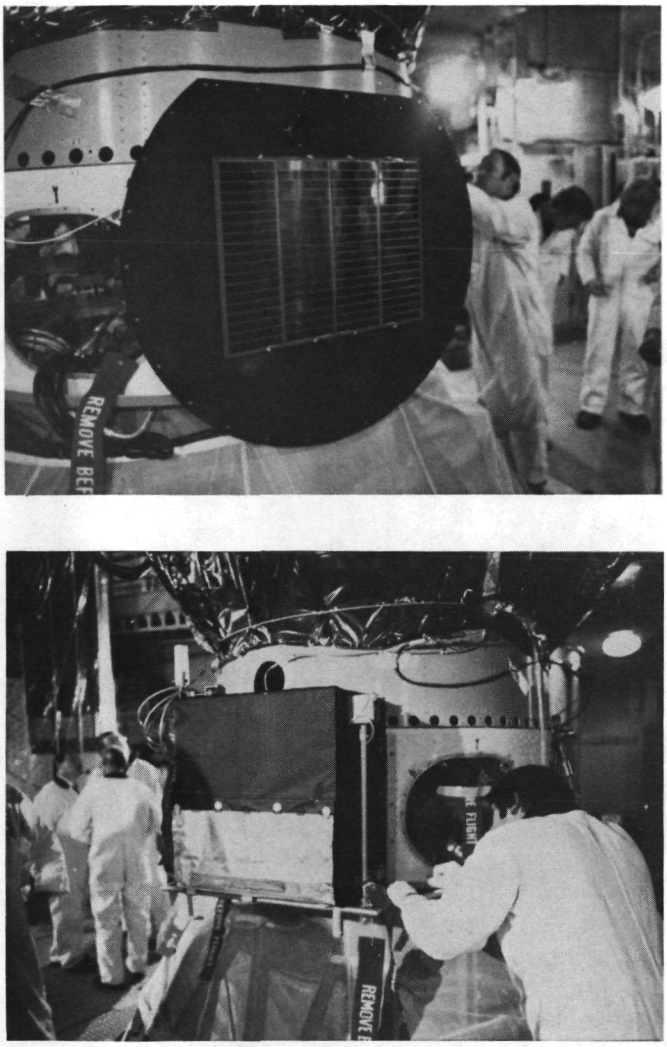

PIX–II installation on Delta second stage, showing solar array and electronics enclosure box

Plasma Interaction Experiment

Electrical interactons between space plasma and spacecraft systems are believed to cause various spacecraft anomalies. Lewis, other NASA Centers, and the Air Force have a coordinated program to explore the interaction phenomena. PIX–II, which was conceived, built, and qualified at Lewis, is part of that program.

Simulating the conditions to be expected on large space systems in low Earth orbit, PIX–II was used to investigate current drains, charge buildup, and discharges to or through the space plasma on various areas (and potentials) of solar arrays. PIX–II was launched on January 25, 1983, as a piggyback experiment on the second stage of a Delta booster that was placed in a 470-nautical-mile orbit. The experiment package consisted of a solar array and sun sensor on one side of the Delta stage and an electronics enclosure box on the opposite side. Two deployable booms held a Langmuir (potential) probe and a hot-wire electron emitter probe.

The experiment data, both stored and real time, were telemetered to Lewis by the Delta downlink and the NASA tracking system. The Air Force received and recorded a significant amount of the flight data obtained and provided tracking station tape data to Lewis for analysis.

The experiment operated successfully, with flight operation extending over 12 orbits (exceeding the planned nine); 38 sucessful tracking station contacts provided about 18 hr of PIX–II data. The data are being analyzed and should furnish investigators with the information needed to understand undesirable and potentially harmful plasma interactions and to devise preventive measures.

Modeling of Propellant Mixing

During missions in space, heat absorbed by cryogenic propellant tanks causes an increase in the tank pressure. One technique for controlling tank pressure is to use a small amount of the cryogenic propellant, evaporated in a cooling heat exchanger, to offset the unavoidable heat addition to the tank. This approach requires the

propellant in the tank to be circulated over the heat exchanger so that the propellant is cooled and mixed.

An experimental program was conducted in the Lewis Zero-Gravity Facility to examine the liquid flow patterns that result from the axial-jet circulation of simulated propellants in model tanks. The effects of the gravity level, the volume of liquid in the tank, the position of the liquid-jet outlet, and the liquid-jet flow rate on the resulting liquid flow patterns were examined.

Four distinct liquid flow patterns were observed under zero-gravity conditions. Dimensionless parameters were developed that characterized the liquid flow patterns and the resulting propellant mixing phenomena. Both the experimental and analytical results are presented in detail in NASA TP-2107.

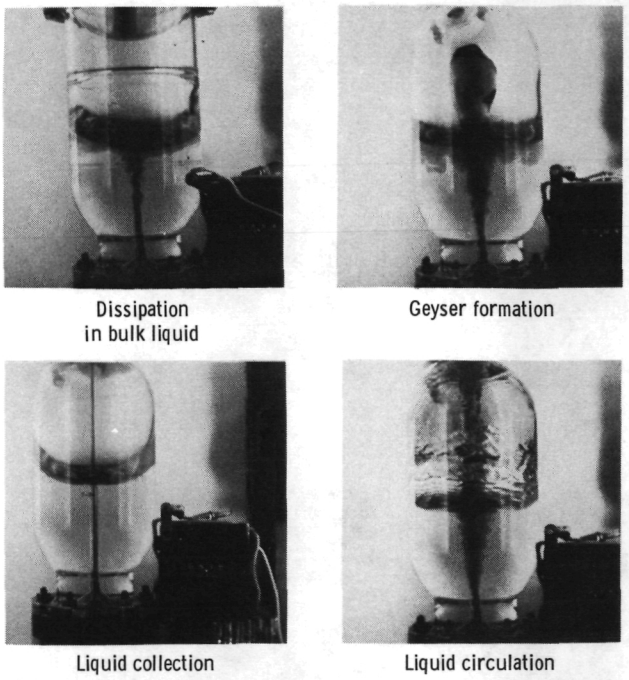

Liquid-jet flow patterns

Resistojet Thruster Evaluations

A resistojet is a type of electric thruster in which electrical energy from an external source is used to heat a propellant that is then expanded to provide thrust. Resistojets are candidates for providing the low-thrust requirements for a space station.

In the high-performance electrothermal hydrazine thruster (HIPEHT) resistojet developed by TRW, the propellant is introduced in a direction perpendicular to the thruster longitudinal axis and tangential to the thruster diameter. The vortex flow field thus established is important to the efficiency of heat transfer between the propellant and the coiled heater that lies on the thruster axis. The heated propellant is expanded through a nozzle optimized for the existing low-Reynolds-number conditions.

An HIPEHT resistojet was evaluated to establish its baseline state-of-the-art performance with propellants such as nitrogen, ammonia, and hydrogen. These propellants are expected to be available on a space station. The tests were conducted by TRW under contract to Lewis. The mass flow rate was varied at the rated heater temperature of 2100° C. Specific impulse was as high as 550 sec with hydrogen. All propellants showed good performance levels even though the unit had been designed for hydrazine. Data and post-test evaluations indicated very efficient energy transfer and compatibility between the

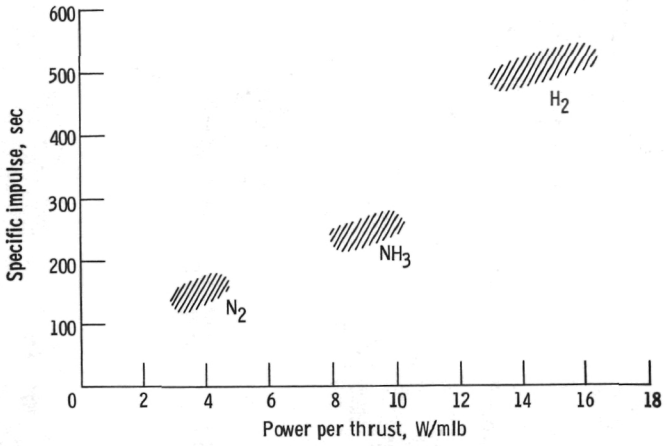

Characterization of HIPEHT thruster

heater and the propellants. Relatively simple redesigns offer promise of improved performance with the candidate propellants. The flexibility of the resistojet concept was demonstrated, and it is a strong contender for a place in a space station auxiliary propulsion system.

Increased Thrust for Ion Propulsion

Studies have shown that ion thruster system mass can be greatly reduced by increasing the thrust density (or thrust per thruster) of ion thrusters. With ion thrusters of present design the thrust density limit, at a given specific impulse, is determined by the maximum ion current density that can be extracted. The ion current density limit is reached when the ion current becomes strongly defocused and impinges directly on the downstream accelerating electrode.

Tests and analyses were conducted at the Jet Propulsion Laboratory under contract to Lewis in order to determine the geometric and operational conditions that result in ion beamlet defocusing and impingement on the downstream accelerating electrode. Data from tests at Hughes Research Laboratories and Lewis were analyzed to obtain information as to the plasma and geometric conditions at the ion accelerator region of the 30-cm-diameter thruster.

The tests and analyses at JPL indicated that increases in the ion current of the baseline 30-cm-diameter thruster are limited by ion beamlet defocusing at a location on the accelerating electrode of about half radius of the thruster. Although the ion current density is significantly less at that position than on axis, the radial translation of the grids with respect to each other (deliberately done to reduce minor thrust losses with the baseline design) causes the ion beam to defocus.

A modified ion accelerator system design, with less grid translation and a prescribed grid spacing, was proposed that would increase the ion current density limit. Tests at Lewis were performed with the new ion optics. The results confirmed the predictions very well; ion current density was increased more than 30 percent. Future systems using these optics will provide higher thrust at lower mass.

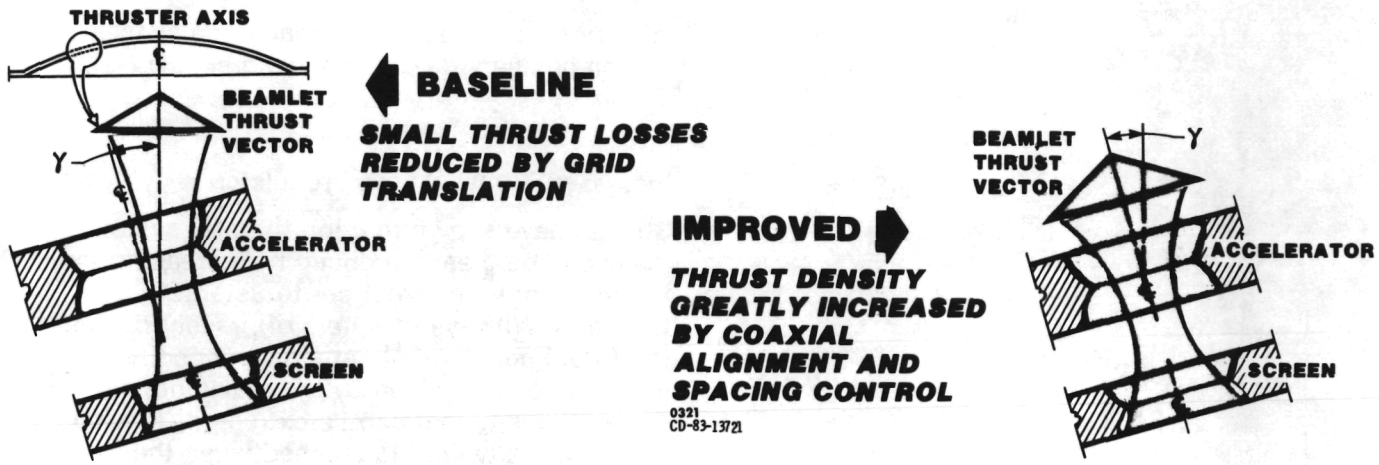

Energy Technology

Iron-Base Alloy for Stirling Engine Cylinder Casting

Stirling engine cylinders must contain the high-temperature and high-pressure (1500° C, 2200 psi) hydrogen working fluid during operation without external cooling. This requires a high-temperature superalloy. HS-31, which contains approximately 55 percent cobalt, is used currently. Cobalt is expensive and scarce and must be imported and is therefore impractical to use for automobile engines. Research was undertaken in support of the Department of Energy–NASA Lewis Automotive Stirling Engine Project to replace HS-31 with a low-cost, low-strategic-material alloy that would still meet the severe operating requirements of the automotive Stirling engine. This work focused on development of a castable alloy composed principally of iron and other low-cost materials such as manganese, aluminum, carbon, and nitrogen. An alloy, presently designated as NASAUT 4G-A1, has been developed. This alloy has high-temperature creep rupture strength and corrosion resistance equivalent to HS-31, and its low-cycle-fatigue life is considerably better. NASAUT 4G-A1 contains neither cobalt nor nickel. Although NASAUT 4G-A1 does contain 15 percent chromium, its high carbon level makes possible chromium

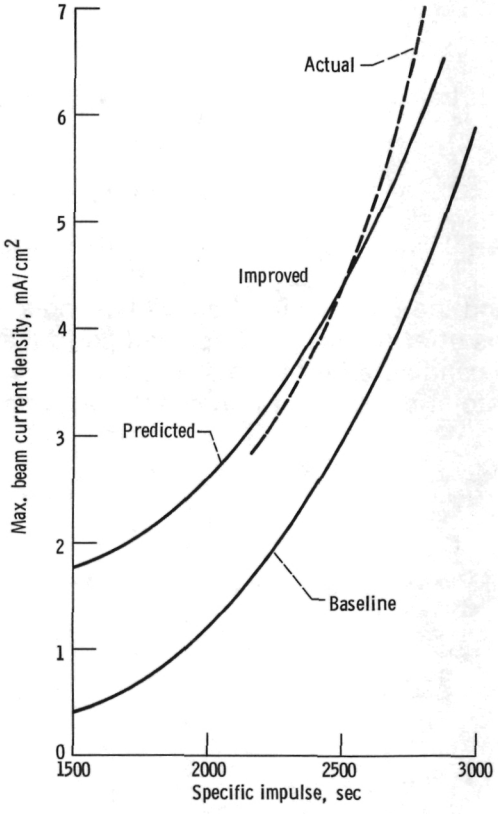

Improved thrust for ion propulsion

addition from high-carbon ferrochromium derived from chromite deposits in the western United States. These chromite deposits had been considered too low grade for stainless steel manufacturers because of their low chromium-to-iron ratios and high carbon content. On this basis, costs for NASAUT 4G-A1 are projected to be only one-twentieth of current HS-31 costs.

Work on this alloy has been confined to laboratory-sized quantities. However, during the coming year a large melt will be produced and extensive testing conducted to confirm that the properties of this alloy can be achieved on a practical basis.

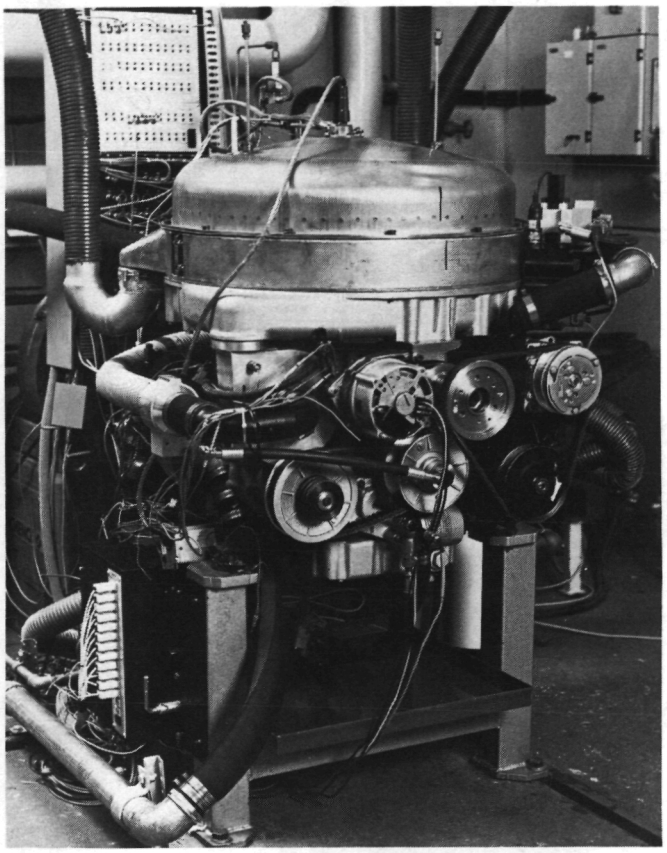

ASE mod I engine

Automotive Stirling Engine Endurance

A major milestone in the Department of Energy–NASA Lewis Automotive Stirling Engine Project was reached when ASE mod I engine no. 3 successfully completed a 1000-hr endurance test on an engine dynamometer. The normal life of an automotive engine is approximately 3500 hr. This engine, which is one of four first-generation engines in the program, has successfully demonstrated nearly one-third of the engine life goal.

During the actual 1002 hr of testing the engine was tested to a duty cycle that was more severe than the standard Federal urban-highway driving cycle. The engine experienced 98 769 cycles of power variation, 12 883 cycles of speed variation, and 229 stop/starts. At the end of 1002 hr the engine was still operating properly and engine performance had only degraded approximately 5 percent from the start of the test. The total accumulated test hours for all four ASE mod I engines in the program was 3469 hr as of 8/26/83.

Stirling Engine Computer Model

The Stirling engine is being developed as a possible alternative to the spark-ignition engine under the Department of Energy's Highway Vehicle Systems Program. Lewis has project

management responsibility for the program. A Stirling engine performance model has been developed at Lewis to support both the project management activities and the Stirling engine test program at Lewis. This model predicts engine performance, including power and efficiency, for a given set of engine operating conditions (such as mean pressure, boundary temperatures, and engine speed). The model has now been documented in a NASA report (NASA TM-82960, 1983) and will be publicly available through NASA's Computer Software Management and Information Center. This is the only publicly available detailed (third order) Stirling model that has been validated for an automotive Stirling engine (the prototype P-40 engine). The documentation includes a users manual for the model and contains all P-40 engine geometrical parameters used in the model.

Endurance Test of a Free-Piston Stirling Linear Alternator System

As part of the first year's effort under a 3-yr cooperative interagency agreement between the Department of Energy and NASA, 600 hr of a planned 1000-hr endurance test have been completed on a free-piston Stirling linear alternator system. This test is being conducted under contract at Mechanical Technology Inc. of Latham, New York, under NASA project management. This type of externally heated engine is a prime candidate for domestic and commercial heat pump applications as well as for space power applications. The attributes of the Stirling system for these applications include potential for long life, high efficiency, and the ability to operate from a variety of heat sources. The 60-Hz, 2.5-kW electric output system operates at a heat source temperature of 700° C under various duty-cycle loads. The engine moving parts are supported on gas bearings that prevent contact with the stationary parts and thus reduce friction and provide high confidence for long-duration maintenance-free operation. This test, which is continuing, is an important step in establishing that the free-piston Stirling engine is a viable candidate for high-efficiency, long-life space power and terrestrial heat pump applications.

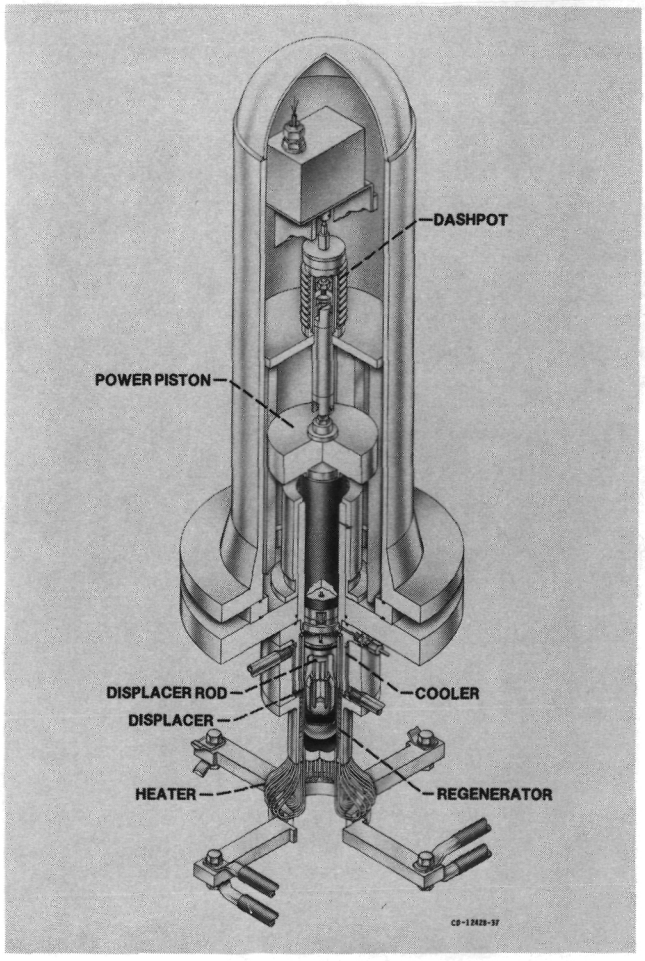

Cutaway of free-piston Stirling linear alternator system

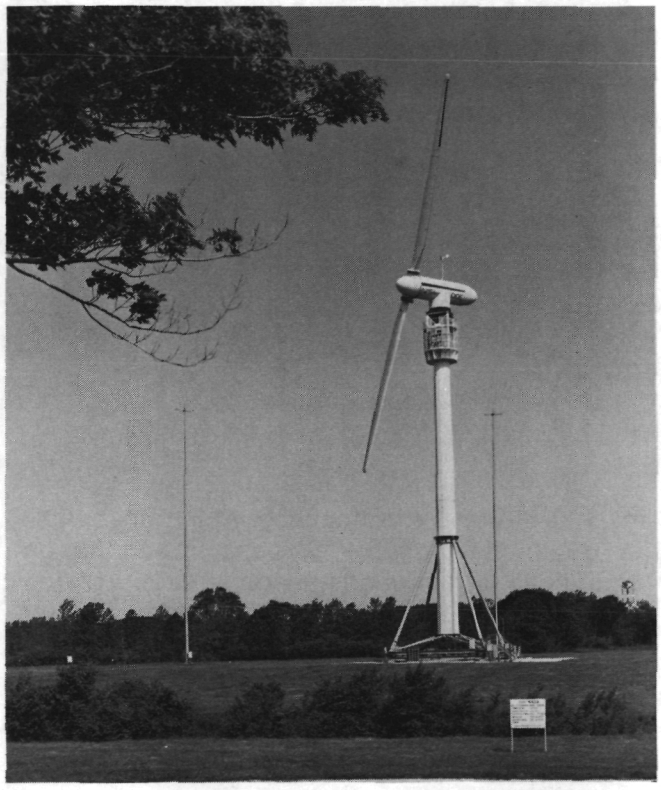

Aileron-controlled blades under test at Plum Brook Station

Enhanced Large Wind Turbine Design

Under the Department of Energy–NASA agreement on large, horizontal-axis wind turbines, Lewis is directing work to improve future wind turbine generator systems. Significant progress is being made in the design and development of aileron rotor control surfaces and variable-speed electrical generators. Both of these developments are expected to improve the performance and reliability and reduce the costs of future large wind turbine generator systems. The results of analytical studies and model testing of various aileron configurations at the Langley Research Center and Ohio State and Wichita State Universities are being confirmed on the Mod-0 research wind turbine at Plum Brook Station.

Variable-speed electrical generators using cycloconverters are under development. A system called the Schleif machine has been tested successfully at Lewis and will be tested on the Mod-0 machine in 1984. A similar concept, under development by the Westinghouse Corporation will also be tested on the Mod-0 machine.

Subject to successful verification of these advanced concepts, aileron controls and variable-speed electrical generators will be incorporated in one or both of the advanced Mod-5 wind turbines currently being designed under parallel NASA contracts by the General Electrical Company and the Boeing Engineering and Construction Company. The General Electric Company and the Hawaiian Electric Company have signed a contract to erect an advanced-design wind turbine (Mod-5A) in Hawaii.

Dynamic control and blade loading tests were conducted on the 2.5-MW wind turbines at Goodnoe Hills. Blade material tests of the fingerjoint concept and material sample testing to establish a strength data base of laminated wood epoxy material for large blade design are continuing.

Advanced Electrocatalysts for Phosphoric Acid Fuel Cell Powerplants

Under a Lewis advanced research contract to develop better electrocatalysts, Giner, Inc., has

developed two catalysts that contain an alloy of platinum and two other metals. Limited tests have shown that these ternary catalysts, when used in a fuel cell cathode, provide a 10-percent improvement in fuel cell performance over an all-platinum catalyst. The output voltages are 55 to 60 mV higher for the ternary catalysts. These output improvements could increase the theoretical efficiency of a fuel cell powerplant from about 45 percent to about 50 percent. The new catalysts would cost substantially the same as the all-platinum catalyst.

Low Cost, Automated Fabrication of Large-Area Phosphoric Acid Fuel Cell Components

The capability to form large, low-cost, porous graphite components for fuel cell electrodes was developed at United Technologies Corporation under a NASA-Department of Energy contract. A commercial double-belt press fabricating machine was modified and adapted for processing fuel cell electrode substrates up to 10 ft^2 in planar area. By using the double-belt press, a labor-intensive process comprising three separate fabrication steps (forming, pressing, and microgrinding) was replaced by one automated process. This process requires only one person to feed raw materials into the machine. The adaptation of this machine is the key element in a more comprehensive NASA-DOE program to advance the development state of electric utility phosphoric acid fuel cells to a precommercial, prototype level.

Gas-Cooled Electric Utility Fuel Cell System

The Westinghouse Electric Corporation under a program jointly funded by the Department of Energy, the Electric Power Research Institute, several participating electric utilities, and Westinghouse itself has developed a conceptual design for a 7.5-MW all-electric prototype fuel cell powerplant. It consists of twenty 375-kW modules, each of which is made up of four 100-kW phosphoric acid fuel cell stacks contained in a pressure vessel that is designed for ease of accessibility and maintenance. A hydrogen-rich gas obtained from a fuel processor operating on natural gas or naphtha is used as the fuel. Air is used as the oxidizer. The whole system operates in a pressurized model, each part being pressurized to complement the fuel cell pressure of 70 psia. The design heat rate is about 8800 Btu/kWh, which is about 39 percent overall powerplant efficiency. In subsequent phases the program effort will progressively advance the fuel cell technology to the program goals, will design and verify system components, and will build, install, and operate two 7.5-MW powerplants at the selected utility sites in 1986-87.

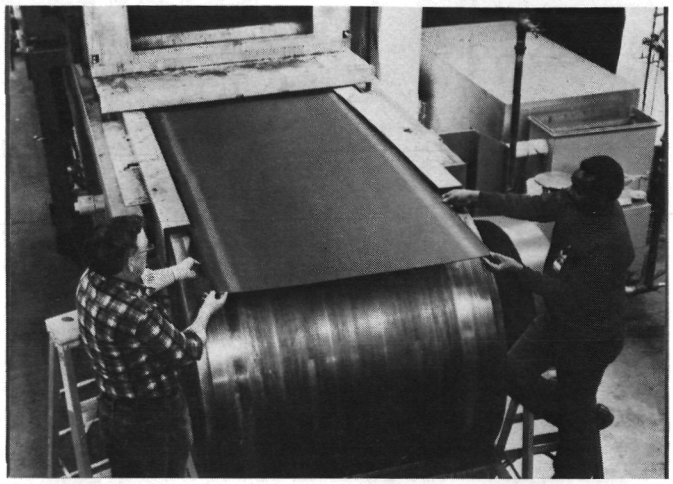

UTC advanced forming process

Title	Lewis contact	Phone number, (216) 433-4000, extension—	Headquarters program office
High-Frequency, High-Power Capacitor	Ira T. Myers	5222	OAST
High-Power, Fast-Switching Transistors and Diodes	Ira T. Myers	5222	OAST
Atomic Oxygen Interaction Studies	Bruce A. Banks	5222	OAST
High-Voltage, High-Power Remote Power Controllers	John C. Sturman	260	OAST
Liquid Droplet Generator	Thaddeus S. Mroz	6144	OAST
Lithium-Counterdoped Solar Cells	Irving Weinberg	5295	OAST
Miniature Gallium Arsenide Solar Cell	Henry B. Curtis	309	OAST
New Design for Individual-Pressure-Vessel Nickel-Hydrogen Cell	John J. Smithrick	364	OAST
"Synthetic Battery Cycling Techniques" Film Supplement	Harold F. Leibecki	5119	OAST
Scaled-Up Water Electrolysis Hardware	Mark A. Hoberecht	6639	OAST
Cryogenic, Long-Life Hybrid Bearings	Ned P. Hannum	5112	OAST
Plasma Interaction Experiment	Louis R. Ignaczak	6652	OAST
Modeling of Propellant Mixing	John C. Aydelott	6612	OAST
Resistojet Thruster Evaluations	Michael J. Mirtich, Jr. James S. Sovey	5192 5183	OAST
Increased Thrust for Ion Propulsion	Vincent K. Rawlin	6664	OAST
Iron-Base Alloy for Stirling Engine Cylinder Casting	William A. Tomazic	258	OAST
Automotive Stirling Engine Endurance	William K. Tabata	6824	OAST
Stirling Engine Computer Model	Roy C. Tew, Jr.	5354	OAST
Endurance Test of a Free-Piston Stirling Linear Alternator System	Jack G. Slaby	6824	OAST
Enhanced Large Wind Turbine Design	Richard L. Puthoff	6106	OAST
Advanced Electrocatalysts for Phosphoric Acid Fuel Cell Powerplants	Robert B. King	6184	OAST
Low-Cost, Automated Fabrication of Large-Area Phosphoric Acid Fuel Cell Components	Paul R. Prokopius	5341	OAST
Gas-Cooled Electric Utility Fuel Cell System	Robert B. King	6184	OAST

Materials and Structures

Simplified Composite Micromechanics Equations

Hygral, thermal, and mechanical (hygrothermomechanical) properties of unidirectional composites are fundamental to the analysis and design of fiber composite structures. Recently, a unified set of composite micromechanics equations was developed at Lewis. The set includes simple equations for predicting ply geometric, mechanical, thermal, and hygral properties by using constituent material properties. In addition, the set includes simple equations for predicting the moisture absorption, the glass transition temperature of the wet resin, and the degradation effects due to hygrothermal environments.

The interrelationships of the equations for each subset geometry, mechanical properties, thermal properties, moisture absorption, and hygrothermal degradation effects are summarized in chart form. This allows the equations for each subset to be on one page for convenience of use and identification of interrelationships.

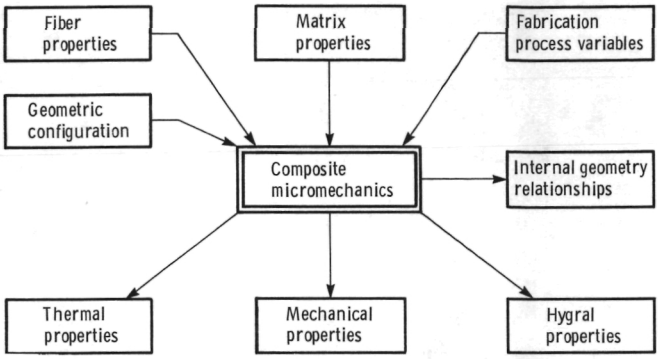

Composite micromechanics definition

INHYD: Computer Code for Intraply Hybrid Composite Design—Users Manual

Intraply hybrid composites have been investigated theoretically and experimentally at Lewis over the past several years. Theories developed during these investigations and corroborated by attendant experiments were used to develop a computer code (program) identified as INHYD (**IN**traply **H**ybrid composite **D**esign). INHYD includes several composite micromechanics theories, intraply hybrid composite theories, and an integrated hygrothermomechanical theory. Equations from these theories are used by the program as appropriate for the user's specific applications.

The theories embedded in INHYD are summarized in recent NASA publications. Instructions for using the program are outlined in a recently completed users manual. The manual provides step-by-step instructions for using INHYD, in both the interactive and the batch modes. INHYD has considerable flexibility and capability, which the user can exercise through the several options described in the users manual. Initially, the manual presents test cases for the interactive mode, first for a dry, room-temperature case and second for a case with moisture present. Then an interactive case is presented wherein the data are preentered, as they would be for a batch case. Next, several cases for using INHYD in the batch mode are described. After following through the test cases presented, a user should be able to use INHYD either in the interactive or batch mode and with or without temperature and moisture effects to predict properties for uniaxial intraply hybrid composites. The users manual also

includes appendixes with (1) a list of elements and subroutines in INHYD; (2) a list of symbols used in the program; and (3) a copy of NASA TM-82593, wherein the theory in INHYD is summarized. It is planned to make INHYD available for public release through COSMIC (Computer Software Management and Information Center).

Simplified Cyclic Structural Analysis Program

A simplified inelastic analysis computer program (ANSYMP) was developed at Lewis for predicting the stress-strain response at the critical location of a thermomechanically cycled structure. This program is intended primarily for use as an economical structural analysis tool in the early design stages of aircraft engine hot-section components, where it would be prohibitively expensive to use nonlinear finite-element analyses. ANSYMP uses as input either a calculated elastic solution for the critical location or a solution constructed from strain measurements. Material cyclic stress-strain and creep properties and creep-plasticity models are coded into user subroutines in the program. The fundamental assumption of the analytical method is that the inelastic strain is local and constrained from redistribution by the surrounding elastic material. An iterative and incremental procedure is used to compute the plastic strains. Creep effects can be calculated on the basis of stress relaxation at constant strain, creep at constant stress, or a combination of stress relaxation and creep accumulation. The simplified method was tested on a number of problems involving uniaxial and multiaxial loading, isothermal and nonisothermal conditions, dwell times at various points in the cycles, and different materials and plasticity models. Good agreement was found between these analytical results and nonlinear finite-element solutions for these problems. The program was also able to predict, to a high degree of accuracy, the cyclic response of thermomechanical fatigue specimens tested under contract. In a typical problem, ANSYMP used less than 1 percent of the computer time required for a nonlinear finite-element analysis.

Resin Selection Criteria for Tough Composite Structures

A new structural methodology has been developed at Lewis for assessing, evaluating, and identifying desirable bulk resin characteristics for specified structural composite integrity (fatigue resistance, fracture toughness, impact resistance, compressive strength, bulking resistance, vibration frequencies, and toughness). The structured methodology is based on an upward integrated mechanistic theory consisting of composite micromechanics, laminate theory, and structural/stress analyses and its inverse (a top-down structured theory). All of these elements are used formally to identify the resin characteristics that have a significant effect on composite mechanical behavior. The structured methodology is based on Lewis' research activities on this subject during the past decade.

The criteria obtained account for resin strength and modulus, ply energy density, laminate first-ply failure, and environmental and cyclic load effects. The criteria are defined in terms of benefit regions for various resin properties, where

the region boundaries are given by simplified equations, or ratios, for resin strength and modulus. The resin selection criteria correlate with experimental data for a variety of conditions including laminate strength and stiffness, high-temperature effects, and resistance to impact. The criteria provide a formalized direction for the a priori selection and development of resins for tougher composites.

Unique Test Method for Determining High-Strain-Rate Properties of Fiber Composites

Testing of fiber composites at high strain rates (dynamic loads) is quite difficult and requires special considerations to assure uniform loading conditions for the specific property to be measured. As a result, several test methods have been proposed, each of which is suitable for only one specific property and is not amenable to complete dynamic characterization including compression, in-plane shear, off-axis loading, and characterization of angleplied laminates.

A unique test method was developed at ITT Research Institute under a contract from Lewis. In this test method ring specimens are loaded by an internal pressure pulse applied explosively through a liquid in a specially designed fixture. This fixture consists of two thick cylinders and two disks assembled together with the ring specimen between them. The reservoir is filled with a mixture of water and water-soluble oil. A pressure pulse is produced in the chamber by detonating an explosive charge in the liquid reservoir. The explosive charge varies according to the laminate layup of the test specimen (or expected failure pressure) and the desired strain rate. Two types of explosive charges were found appropriate: pistol powder in quantities from 260 to 1569 mg, and PETN detonators (50, 100, and 330 mg). The explosive amounts can be varied with the various specimens to obtain a range of strain rates.

The ring specimens are instrumented with suitable strain gages to measure the strain as a function of time. The pressure in the ring is

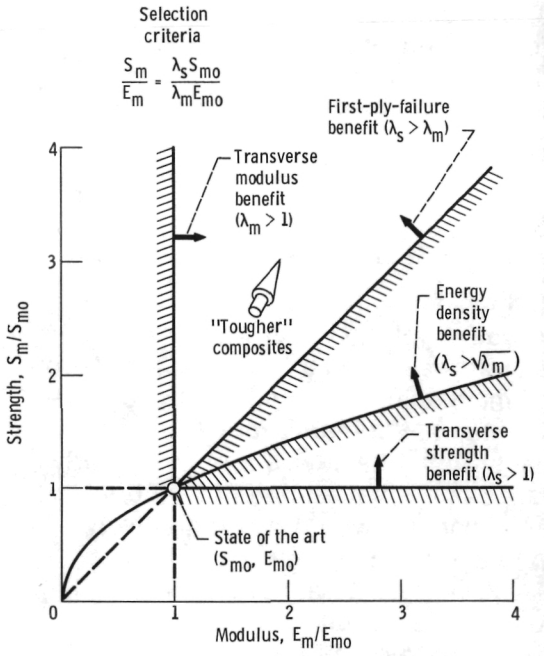

Resin selection criteria for tougher composites

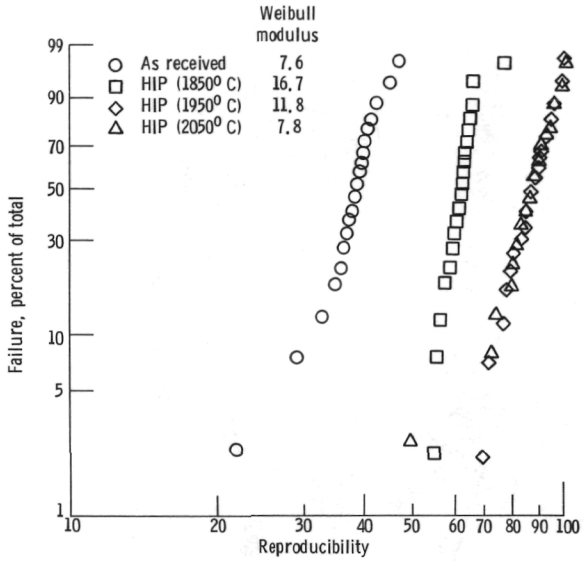

Improved reproducibility of reaction-bonded Si_3N_4 with hot isostatic pressing

determined from the strain in a steel calibration ring. The steel ring is fabricated from Vascomax steel. The large amount of dynamic data generated during testing is acquired and processed on a dedicated microprocessor with special firmware.

Ultrasonic Ranking of Tungsten Carbide Toughness

Reduced expense and improved reliability can be realized by using nondestructive methods to verify the mechanical properties of materials that are usually subjected to destructive testing procedures. For example, the usual method for determining fracture toughness involves the fabrication and subsequent fracture of material samples. In the case of cobalt-cemented tungsten carbides this process requires considerable time and expense because of difficulties in machining appropriate samples. Consequently, a simpler, less costly procedure called the Palmqvist method was devised as an alternative. However, the Palmqvist method requires the introduction of microcracks. In addition to being time consuming the Palmqvist method is not truly nondestructive and hence cannot be applied to articles destined for actual use. The toughness of cemented carbides is of great importance in the manufacture of high-performance machine tools.

A feasibility study was conducted at Lewis to determine if nondestructive ultrasonic measurements could be used to rank tungsten carbide alloys according to fracture toughness. Toughness was mechanically determined for six tungsten carbide alloys varying from 2 to 16 wt% cobalt. The toughness generally increased with increasing cobalt content. A Lewis-developed pulse-echo ultrasonic technique was then applied, and an ultrasonic attenuation factor was calculated for each alloy. A strong linear correlation was found between the ultrasonic attenuation factor and toughness previously measured by the Palmqvist method. Typically, as the amount of ductile cobalt binder phase increased, toughness and ultrasonic attenuation also increased. Clearly, the ultrasonic approach is a nondestructive alternative to mechanical, destructive methods for ranking the toughness of cemented carbides.

Hot Isostatic Pressing of Ceramics

High-temperature SiC and Si_3N_4 ceramics are currently being considered for structural components in advanced turbines. They offer very

attractive improvements in efficiency through the use of higher engine operating temperatures without cooling. The major drawback to using ceramic materials is that they currently have a wide distribution in strength due to minute processing flaws, such as voids, which are extremely difficult to prevent.

One technique to reduce this void population is hot isostatic pressing (HIP). Commercial SiC and Si_3N_4 materials were obtained and subjected to 2000-psi pressure at high temperatures (1850° to 2200° C). This reduced both the size and number of voids present. Probability-of-failure plots showed that hot isostatic pressing increased the average strength of both materials and was especially effective in eliminating the low-strength distribution. The Weibull modulus (a measure of the reproducibility of the material) can be significantly improved by judicious use of this technique. This is an important consideration for ceramics, which normally suffer from lack of reproducibility. It is expected that further improvements could be made by directly hot isostatic pressing powders that have not been previously fully sintered.

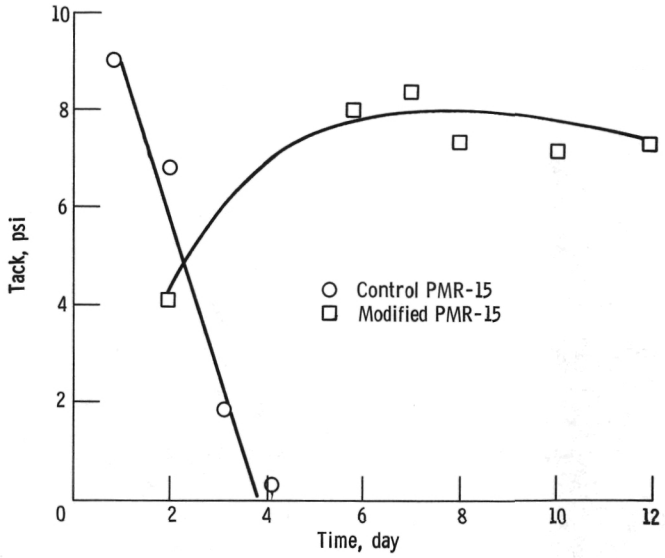

Improved tack of PMR-15 impregnating materials

Improved PMR-15 Polyimide

The high-temperature resin known as PMR-15 (**P**olymerization of **M**onomer **R**eactants) polyimide was developed at Lewis in response to the need for processable, high-temperature-resistant matrix resin for fiber-reinforced composites. This resin is finding growing use in military and commercial aircraft engines. Current-technology PMR-15 consists of a monomer reactant mixture containing the monomethyl ester of 5-norbornene-2,3-dicarboxylic acid (NE), the dimethyl ester of 3,3',4,4'-benzophenonetetracarboxylic acid (BTDE), and 4,4'-methylenedianiline. Solutions to impregnate reinforcing fibers are generally prepared by dissolving the monomer mixture in methanol. Although the volatility of methanol is highly desirable for obtaining void-free composites, it does limit the tack (stickiness needed for component fabrication) and drape-retention characteristics of unprotected

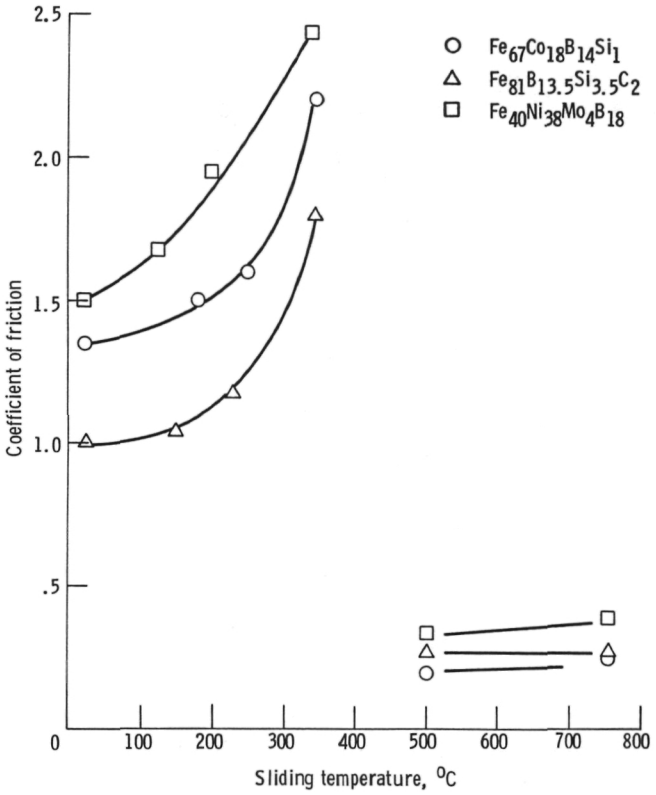

Coefficient of friction as a function of temperature for aluminum oxide sliding on ferrous-base metallic glasses in vacuum

impregnating materials exposed to air and thus reduces fabrication flexibility.

PMR-15 monomer reactants and a mixed solvent have been identified that provide impregnating materials with improved tack and drape-retention characteristics without changing their basic chemistry or processability. The modifications consist of substituting higher alkyl esters for the methyl ester in NE and BTDE and using a solvent mixture (3:1 methanol/1-propanol) in lieu of pure methanol. The ester and solvent modifications extended the tack and draft retention of PMR-15 impregnating material to beyond 12 days under ambient conditions. The improved-tack PMR-15 system should facilitate the fabrication of large, complex structures that require long layup times and should provide cost savings because of reduced material scrap.

Tribological Properties of Amorphous Alloys

Research at Lewis has identified a new class of materials with potential for high-temperature bearing applications. X-ray photoelectron spectroscopy (XPS) analysis, transmission electron microscopy, diffraction studies, and sliding friction experiments have been conducted to determine the surface chemistry, microstructures, and friction properties of ferrous-base metallic glasses at temperatures to 750° C. Sliding friction experiments were conducted in ultrahigh vacuum with three ferrous-base metallic glasses in contact with an aluminum oxide rider at temperatures to 750° C.

The results of the investigation indicate that the relative concentrations of the various constituents at the surface of the sputtered specimens are very different from the normal bulk compositions. Contaminants can come from the bulk of material to the surface upon heating and impart boric oxide and silicon oxide at 350° C and boron nitride above 500° C. The coefficient of friction increased with increasing temperature to 350° C. Above 500° C the coefficient of friction decreased rapidly. The segregation of contaminants is responsible for the friction behavior.

Universal Binding Energy Curve

Fundamental analytical studies of the binding of solid surfaces have resulted in the development of a univeral relationship to predict bonding of molecular chemisorption species and metal-to-metal adhesion without having to conduct difficult experimental tests. An earlier investigation established the ability to predict adhesive behavior for like and dissimilar metals in contact. The theory was extended to include not only metals in contact, but also the processes of gaseous species residing on a solid surface as well as those chemically interacting with the surfaces by chemisorption. A clear universal relationship exists for binding energy as a function of separating distance.

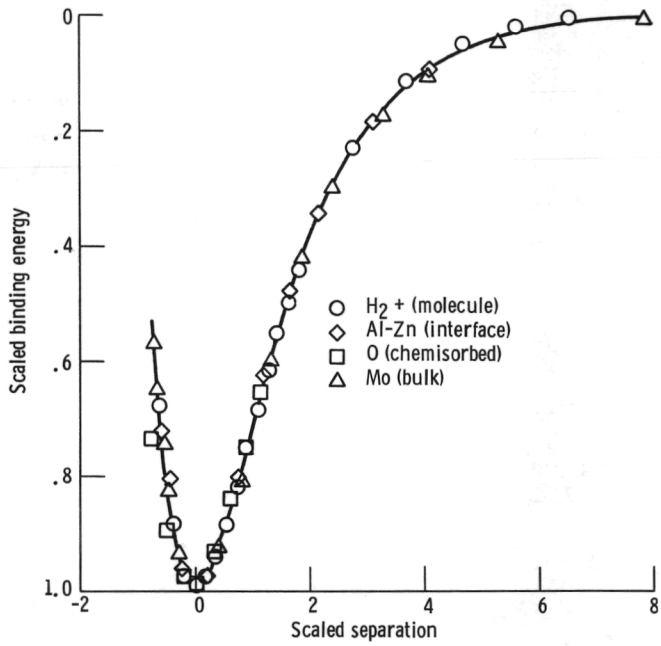

Binding energy as a function of separating distance

Ball Bearing Thermal Analysis

An analysis to calculate the thermal performance of ball bearings has been developed. The analysis has been verified by comparing predicted performance with experimental data from three sizes of angular-contact ball bearings. The thermal variables used for comparison were bearing temperature, oil-out temperature, and bearing heat generation.

An equation was derived to determine the percentage of bearing cavity volume that is occupied by lubricant. This factor describes the density of the lubricant-air mixture and is used primarily for calculating ball drag, a significant source of heat generation in liquid-lubricated ball bearings. This equation was verified and ball bearing thermal performance was predicted over a range of bearing sizes, shaft speeds, and lubricant flow rates. Bearing heat generation of the three angular-contact bearings correlated well with the speed parameter DN. (DN is the product of the bearing bore diameter in millimeters and the shaft speed in rpm.)

Finite-Element Analyses of Sliding Surface Temperatures

Frictional heating of sliding systems increases the temperatures of the sliding bodies, especially in the immediate region of the contact interface. The temperature on the contact surface can be high enough to have a considerable influence on the performance of the sliding system. Because of this, it is important to be able to predict

surface temperatures in sliding contacts. A number of techniques have been developed for surface temperature analysis, but none have proven universally adaptable because of their mathematical sophistication or their inapplicability to bodies of finite dimension. The finite-element method suffers from neither of these restrictions.

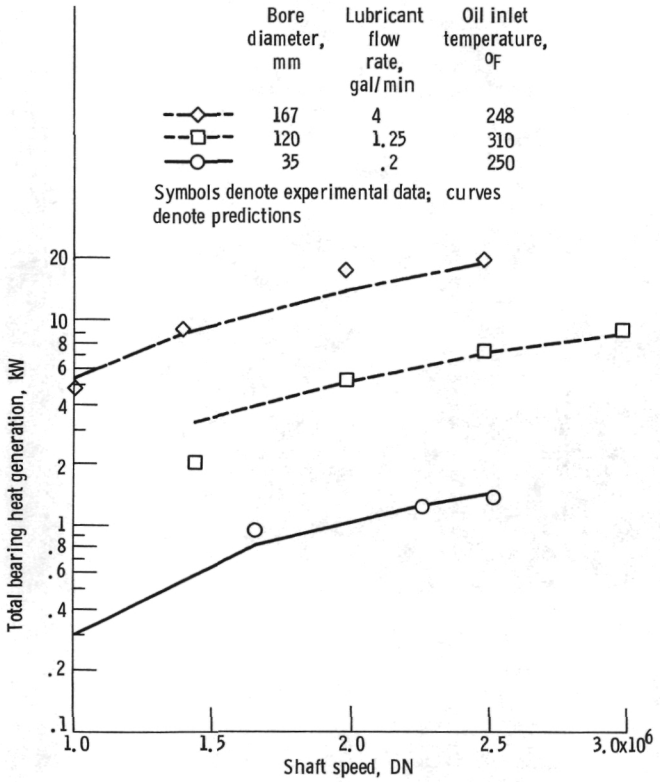

Comparison of experimental and predicted heat generation

A finite-element program was developed specifically for analyzing surface temperatures in sliding systems. The program can model heat conduction in two-dimensional or axisymmetric three-dimensional bodies with known convection, heat flux, or prescribed temperature boundary conditions. It can be applied to bodies that are either moving or stationary with respect to a source of frictional heat or to systems composed of both types of bodies. The analysis may be steady state, quasi steady state, or transient, and in the latter case, boundary conditions, frictional heat generation rate, and velocity may all be functions of time. Properties of the contacting materials may be temperature dependent.

Although the program was originally developed for studying temperatures in turbine engine gas path seal rubs, it has found application in a variety of sliding components, including sleeve bearings, face seals, and disk brakes. The program's capabilities were proven by comparison with closed-form solutions for a dozen different problems and by application to systems for which experimental temperature measurements were available. Numerical inaccuracies in the solutions for moving body cases or transient solutions have been characterized and guidelines have been developed for their avoidance. The program has been well documented and an instruction manual has been written to give a step-by-step procedure and explain program operation.

Analysis of Traction Characteristics of Lubricants

The knowledge of the traction characteristics of a lubricant is of engineering importance in the design of many machine elements, such as bearings, gears, cams, and particularly traction drives. The effective traction coefficient occurring in the contact dictates the amount of slip in ball bearings, the skew in roller bearings, and the creep rate across a traction-drive contact. The product of the traction force and slip rate is also a direct measure of the load-dependent power loss of a rolling-element contact.

The traction coefficient is the single most important parameter in determining the life, size, and performance of traction drives. The fatigue life of a traction-drive contact has been theoretically shown to be proportional to the cube of the coefficient of traction for a given size and a constant torque level. It has also been shown that the size of the traction drive is inversely proportional to the coefficient of traction to the 0.36 power.

Simple equations were developed that allow the designer to readily determine the maximum allowable traction coefficient and initial traction curve slope at most operating conditions for two leading traction fluids. The agreement between predicted and measured traction coefficient data was quite good. The information provided by the analysis is critical to optimizing the performance of traction drives and similar devices.

IR-100
System for High-Speed Balancing of Shafts

Lewis and Mechanical Technology Inc. of Latham, New York, have jointly developed a microprocessor-controlled laser balancing system. This system is the outgrowth of several years sponsorship by NASA of programs to develop balancing methodology. It combines the influence coefficient balancing method with automatic material removal by a pulsed laser.

In the influence coefficient method of shaft balancing, trial weights are applied to the shaft; the resulting change in vibration characteristics, when divided by the trial weight, determines an array of sensitivity factors, or influence coefficients. From the influence coefficients and the measured shaft vibration, balance corrections are calculated that will minimize the residual shaft vibration. The calculations are all performed by the microprocessor. When balancing a number of shafts of the same design, influence coefficients can be stored in the system; they need not be reacquired for each shaft.

Balance corrections are made by removing material from the spinning shaft with a pulsed laser; control circuits fire the laser at the appropriate time to hit the proper angular location on the shaft. The laser can also be used to apply trial weights when acquiring influence coefficients.

Microprocessor-controlled laser balancing system

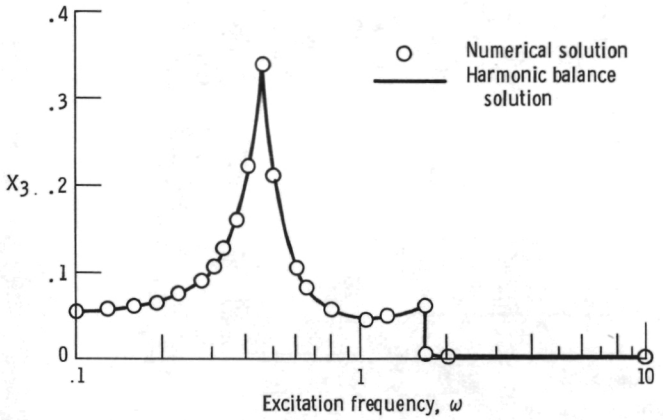

Amplitude and phase relationship of third harmonic component for large nonlinearity

The microprocessor system is compatible with commercially available balancing machines. Alternatively, in-place balancing can be performed; all that is required is vibration information from the shaft via displacement sensors or accelerometers. Different models of pulsed lasers (typically neodymium-glass or neodymium-yttrium-aluminum-garnet (YAG)) can be used, depending on the material removal rate desired.

Lewis and MTI jointly received an IR-100 award for this system.

Solution of Nonlinear Coupled Differential Equations by Harmonic Balance Method

The complete equations of motion for geared shaft systems contain nonlinear terms. Although these terms are commonly neglected in rotordynamic calculations, order-of-magnitude analysis indicates that they are significant in geared shaft systems. Up to now, suitable techniques have not been available for solving the complete nonlinear equations. However, the method of harmonic balance has recently been shown to be a suitable solution technique. Moreover, the method is usable with transfer matrices, which are commonly used to analyze shaft systems. The solution to the nonlinear equation, with a periodic forcing function, is represented as the sum of a series similar to a Fourier series but with the form of the terms suggested by the equation itself. As an example, consider the equation for a single-degree-of-freedom spring-mass system with a nonlinear spring

$$MX + d(X + \epsilon X3) = F \sin \omega t \qquad (1)$$

The solution to this equation is taken to be

$$X = X_1 \sin \omega t + X_3 \sin 3\omega t + \text{Higher order terms}$$

This expression is substituted in the differential equation. If all higher order terms are neglected (i.e., only terms in sin ωt and sin $3\omega t$ are retained), the differential equation is reduced to a pair of simultaneous nonlinear equations in X_1 and X_3. Using a two-dimensional Newton-Raphson technique yields X_1 and X_3.

Results of this work were compared with a numerical solution of equation (1). Fourier

analysis was used on the numerical solution to yield the various frequency components; the value of the X_3 term is shown in the accompanying figure for a large nonlinearity ($\epsilon = 1$) and for a range of excitation frequencies ω. The results of the harmonic balance method are virtually identical to the numerical results. For this particular case the Fourier analysis of the numerical results showed that all frequency components other than X_1 and X_3 were at least an order of magnitude less than X_3; thus the overall solution accuracy is excellent. The harmonic balance method has been applied to a coupled two-degree-of-freedom spring-pendulum system with equally good results.

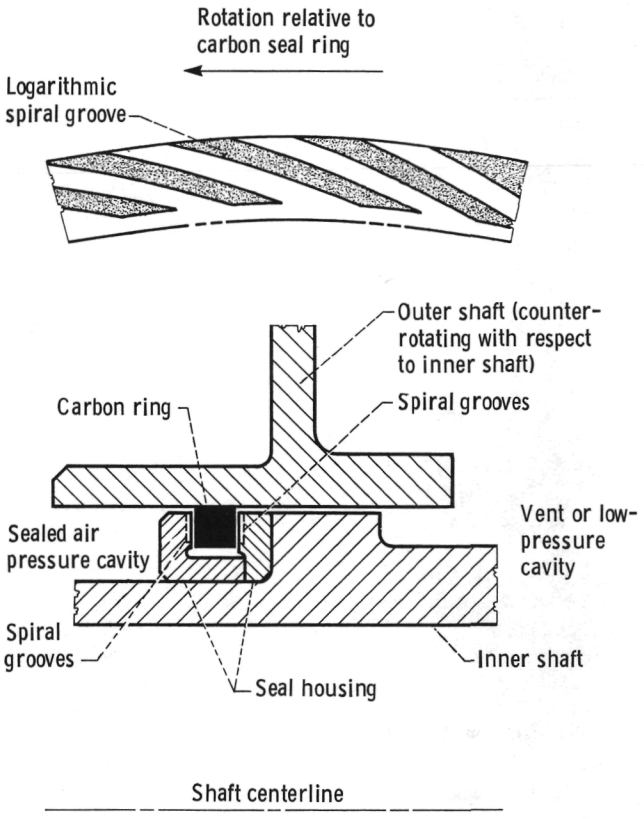

Spiral-groove intershaft ring seal and spiral-groove geometry

Dynamic Analysis of Multiple-Shaft Systems

A computer code has been developed for the transient response of flexible shaft systems, such as those in turbine engines. The transient response must be known to properly account for suddenly applied forces, such as blade loss and seal rubs. In multiple-shaft systems, forces applied to a shaft can have a large effect on the other shafts of the system. Early shaft analyses used a lumped-mass, direct integration approach. With the large number of masses required to model a multiple-shaft system, numerical instability all but precluded transient response calculations. Model methods, such as component mode synthesis, circumvent this by basing calculations on natural modes of the shaft. Generally, only a small number of modes need be used—typically three or four for each shaft—whereas each shaft may be modeled with 20 or more mass stations.

Component mode synthesis operates by first calculating static constraint modes, or the modes in which the shafts do not rotate. The modes are calculated by prescribing a unit displacement at each bearing in turn, with zero displacement prescribed at the remaining bearings. These modes are then combined with constrained normal modes, which are whirl modes having zero displacement at all bearings. The resulting combination accurately depicts actual rotor motions: since the normal modes are calculated for a particular speed, they account for gyroscopic effects more efficiently than analyses using "free-free" modes.

The computer program that implements the analysis is quite versatile, yet program input is straightforward. Input follows the usual form for rotordynamic codes with shaft diameter, length,

density, and elastic modulus given for each shaft element. Linear or nonlinear bearings can be modeled, with bearings connected either to ground or another shaft. Program output can include damped whirl speeds and mode shapes, steady unbalance response, and transient response to maneuver loads or blade loss.

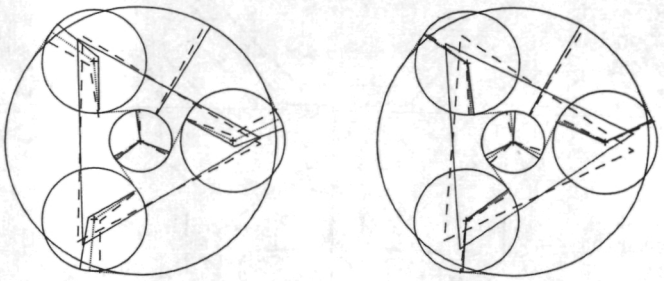

Vibration in planetary gear systems—computer graphics

Spiral-Groove Ring Seal for Counterrotating Shafts

The spiral-groove intershaft ring seal is a new seal concept that has potential application in sealing fan bleed air between two counterrotating shafts in advanced turbofan aircraft engines. This is a difficult sealing application for any contacting seal because the counterrotating shafts set up very high sliding speeds for the seal, of the order of 850 ft/sec. In addition to the high sliding speed the seal must accommodate approximately 0.25 in. of axial translation due to relative axial motion between the two shafts.

Applying a self-acting geometry in the form of spiral grooves to the faces of the ring seal housing will maintain a thin air film of relatively high stiffness between the seal ring and the housing and thus allow the seal to operate in a noncontacting mode over the entire engine operating range. The seal can then operate at a sliding speed of 850 ft/sec, can accommodate axial translation of 0.25 in., and can have leakage rates comparable to those of contacting seals.

When spiral grooves are employed in a seal as a film-generating mechanism, calculating the axial force equilibrium generally requires

(1) Film-load capacity curves (lift force as function of film thickness)
(2) Minimum film thickness over the operating range
(3) Optimization of the spiral-groove geometry to maximize the lift force for a given seal envelope size and operating condition

A Lewis-developed computer program was employed to analyze the performance of the spiral grooves for the counterrotating ring seal application.

Vibration in Planetary Gear Systems

An algorithm suitable for a minicomputer was developed for finding the mode shapes and natural frequencies of a planetary gear system. Mode shapes are presented as graphical computer output. Excellent agreement was obtained between natural frequencies calculated by assuming constant mesh stiffnesses and resonant frequencies obtained by integrating the equations of motion. The methodology is a quick and efficient means of identifying operating resonance regions and analytically tuning the drivetrain by examining the effect of such parameters as planet and sun gear support stiffnesses, input-output shaft stiffnesses, and gear mesh stiffnesses. The graphical output provides dramatic visual aid for understanding vibrational modes.

Optimized Eddy Current Rotor Damper Design Analyses

An expression for the amount of damping available in an eddy current damper has been determined, and the underlying physics of eddy currents and permanent magnet systems has been investigated. The eddy current damping coefficient is inversely proportional to the resistivity of the conductor materials used and is directly proportional to the magnetic field that the moving conductor passes through and the relative velocity between the conductor and the permanent magnet. The design of magnetic circuits using permanent magnets to provide the necessary field requires special consideration. Computer programs to investigate different permanent magnet geometries have been developed to assess geometry effects on the eddy current damping coefficient.

A highly optimized and idealized conceptual eddy current damper design has been developed. The concept is somewhat different from the one currently under study for application to the space shuttle main engine. The U-shaped alnico magnet is the heart of the damping mechanism. The magnet is shaped to capture and use the fringing flux. The rare-earth pole pieces provide extra flux to the magnetic circuit; they are beveled to concentrate and direct the magnetic flux. The high-purity copper conductor is shaped to capture fringing flux as well as gap flux for eddy current production. The upper alnico magnet is attached to the copper conductor, and the assembly would be affixed to the bearing support of a rotor in a turbomachine. The pole faces of this magnet oppose those of the larger alnico magnet and provide static stiffness to this mechanism as a result of magnetic repulsion. The displacement-versus-force curve is parabolic, with increasing stiffness with displacement. The upper alnico magnet produces a demagnetizing force on the larger alnico magnet, but this has a small effect since rare-earth pole faces are used that have a high coercive force and can resist a high demagnetizing force. When this mechanism is immersed in liquid hydrogen, the resistivity of the pure copper conductor decreases and the damping coefficient increases, both by a factor of 100. This mechanism can provide a damping coefficient upwards of 100 lb sec/in. in liquid hydrogen. Eddy current dampers using permanent magnets can be relatively uncomplicated, small, lightweight, and highly effective in cryogenic turbomachine applications.

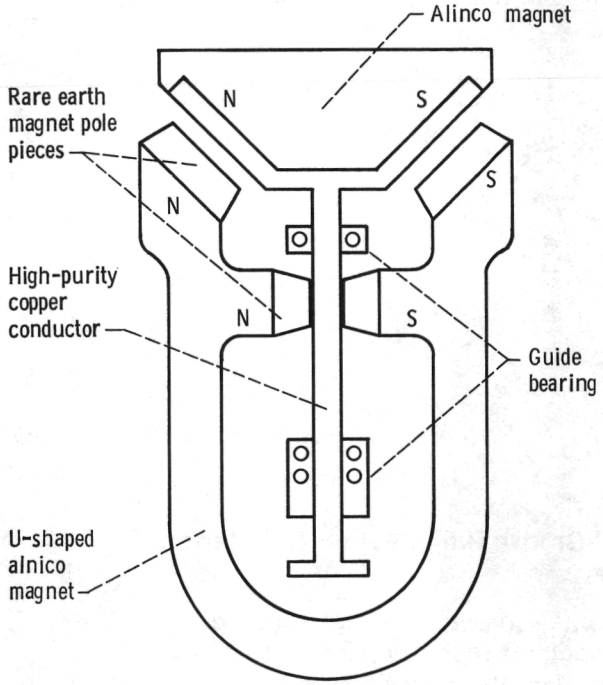

Schematic of eddy current damper design with magnetic repulsion stiffness

Elastomeric Dampers for Rotating Machinery—Design Handbook

A design handbook for elastomeric dampers, which have a number of advantages over other types of dampers, has been developed. Elastomeric dampers are comparatively inexpensive and easy to manufacture and assemble. They can handle shock and moderate overloads and tolerate substantial misalignment. Because they provide both stiffness and damping in a single element, they obviate the need for the parallel stiffness elements required in most conventional rotordynamic squeeze-film damper assemblies. A typical elastomeric damper design is shown in the accompanying figure. The simplicity and compactness of this particular design are quite apparent. This elastomer-damped support performed effectively on a high-speed turbine shaft balancing rig that was intentionally operated through two bending critical speeds.

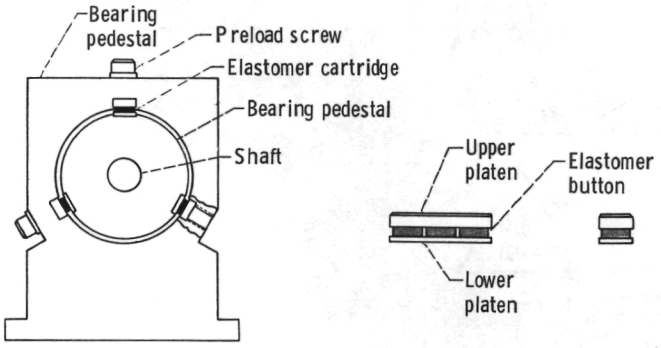

Arrangement of elastomer cartridges

Cartridge construction with three buttons

Elastomer damper construction

The design of the elastomer cartridges followed a step-by-step procedure as given in the design handbook specially developed for these devices. The specific elastomer types for which dynamic properties are given in the handbook are polybutadiene, 70- and 90-durometer Viton (fluorocarbon elastomer), Buna-N, EPDM, and neoprene. Other physical properties of these and many other types of elastomers are also presented in the handbook. These physical properties include density and thermal conductivity. An extensive list of references, for a wide variety of elastomer types, is also given.

Empirical data were obtained through extensive testing of several different engineering elastomers. Dynamic properties, such as the stiffness and damping, of many of these viscoelastic materials were not previously available over the frequency range of interest for rotating machinery. Experiments conducted with elastomers in compression and shear loading disclosed that stiffness and damping vary more significantly with the amount of strain than with frequency.

Structural Tailoring of Engine Blades (STAEBL)

One of the more difficult tasks in the development of aircraft gas turbine engines is the aerostructural design of fan and compressor blades. After an aerodynamic design is selected, the blade must be structurally designed to satisfy constraints on steady-state and vibrator stresses, flutter, local and root foreign object damage, and engine-order resonance. Because of the diverse nature of these constraints and the inherent

complexity of blade designs, the design process is very iterative and is strongly controlled by experience and subjective judgment. As a result, once an acceptable design is found, it is frequently considered to be final even though significantly better designs may be possible.

To improve the overall structural design process, Lewis contracted with Pratt & Whitney Aircraft Company to develop and demonstrate an automated approach based on standard structural analysis methods and optimization techniques. The key elements of the procedure are (1) approximate analysis methods to reduce the total computational effort and (2) the optimization technique. Both elements are used in an inner loop to find a candidate design that meets structural constraints and minimizes the selected objective function. A scaling procedure was also incorporated so that the blade chord could be changed while maintaining the basic aerodynamic design. In developing this program an established optimization procedure, COPES/CONMIN, was used. The objective function was direct operating cost plus interest for an entire aircraft. After a candidate design was found, it was analyzed with refined analyses to verify that all constraints had been met. Currently, an effort is under way to improve the approximate local foreign object damage and stress analyses and to deliver a nonproprietary computer code containing the optimization procedure and all approximate analyses.

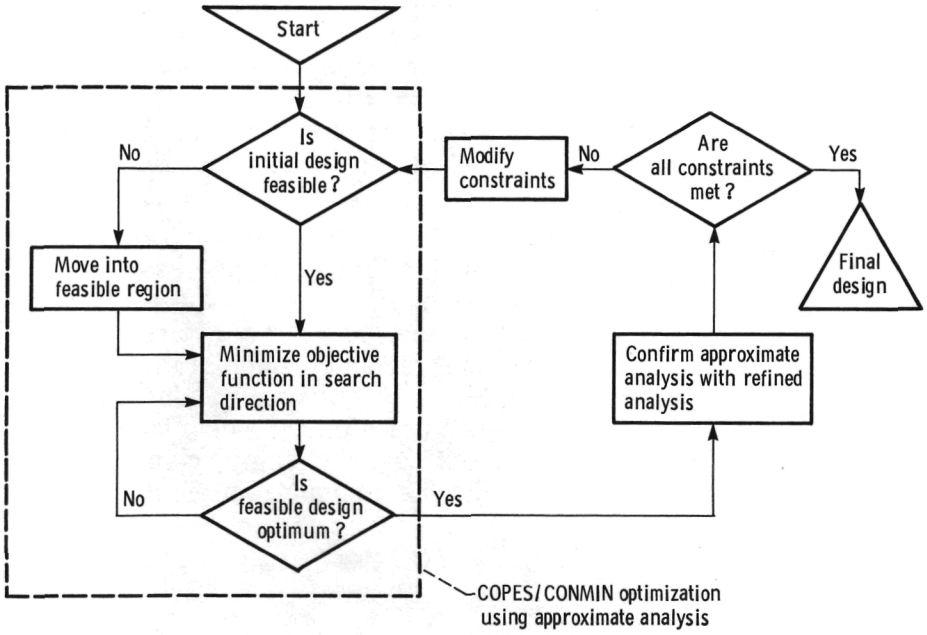

Procedure for structural tailoring of engine blades

Vibration Prediction for Twisted Blades

A cooperative study by government, industry, and academia has yielded a data base that should result in improved methods of designing turbine engine blades. It has been suspected that many methods in use for predicting the natural resonant frequencies of blades do not yield accurate results for very highly twisted blades. Thus interested groups were asked to use various predictive methods on a chosen set of blade geometries and to submit results for comparison with each other and with experimental results. The theoretical results were generated by various finite-element, shell, and beam analysis methods. The experimental results were obtained from a set of precision-machined blades tested at two laboratories. The comparison showed clearly which methods yield good accuracy. Most methods yielded reasonable agreement with experimental results, especially for modest twist. But one popular method was shown to be inadequate for highly twisted blades.

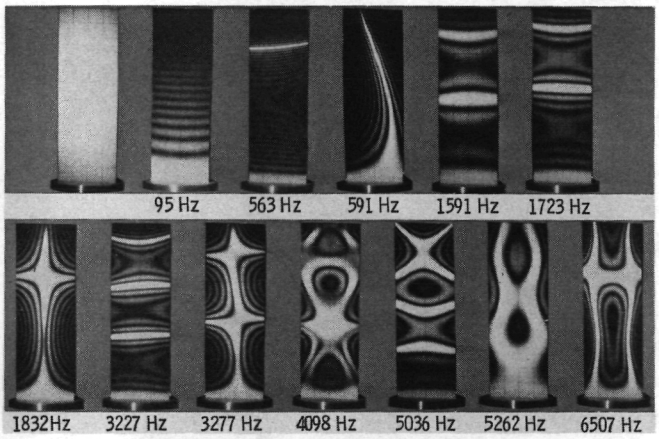

Holography-produced accurate values of resonant frequencies and displacement contours

Hot, Wet Compression Fatigue Behavior of Composites with Defects

The fatigue resistance of fiber composite laminates with defects and subjected to the hot, wet environments typical of turbine engines needs to be determined so that life and durability can be properly addressed during the design phase.

An experimental program was conducted by Boeing under a contract from Lewis to investigate the effects of moisture and high temperature on the fatigue and fracture response of composite laminates under compression loads. The structural laminates investigated were a typical angleply laminate and a typical turbine-engine fan blade laminate. Defects investigated were full- and half-penetration slits and impact delaminations. Experimental results were obtained showing
(1) the effects of moisture on the fracture and fatigue strength at room temperature, 394 K (250° F), and 422 K (300° F); (2) the effects of defect size and type on the compression-fracture strength under moisture and thermal environments; and (3) the fatigue lives and residual-compression strength under compression only and under tension-compression fatigue loading.

The results show that (1) high temperature significantly degraded compression fracture strength, with the hot, wet environment being the most degrading; (2) full-penetration slits were the most critical of the defects studied (more so than half-penetration slits, implanted disbonds, and impact damage); and (3) impact-induced delaminations were as critical as slits.

Title	Lewis contact	Phone number, (216) 433-4000, extension—	Headquarters program office
Simplified Composite Micromechanics Equations	Christos C. Chamis	6831	OAST
INHYD: Computer Code for Intraply Composite Design—Users Manual	Christos C. Chamis	6831	OAST
Simplified Cyclic Structural Analysis Program	Albert Kaufman	5143	OAST
Resin Selection Criteria for Tough Composite Structures	Christos C. Chamis	6831	OAST
Unique Test Method for Determining High-Strain-Rate Properties of Fiber Composites	Christos C. Chamis	6831	OAST
Ultrasonic Ranking of Tungsten Carbide Toughness	Alex Vary	357	OAST
Hot Isostatic Pressing of Ceramics	Michael L. Millard Gordon K. Watson	5362 434	OAST
Improved PMR-15 Polyimide	Raymond D. Vannuci	6967	OAST
Tribological Properties of Amorphous Alloys	Kasuhisa Miyoshi	5271	OAST
Universal Binding Energy Curve	John Ferrante	5203	OAST
Ball Bearing Thermal Analysis	Richard J. Parker	6672	OAST
Finite-Element Analyses of Sliding Surface Temperatures	Albert F. Kascak	6950	OAST
Analysis of Traction Characteristics of Lubricants	Stuart H. Loewenthal Douglas A. Rohn	6839 6839	OAST
System for High-Speed Balancing of Shafts	David P. Fleming	6975	OAST
Solution of Nonlinear Coupled Differential Equations by Harmonic Balance Method	David P. Fleming	6975	OAST
Dynamic Analysis of Multiple-Shaft Systems	David P. Fleming	6975	OAST
Spiral-Groove Ring Seals for Counter-rotating Shafts	Eliseo DiRusso	6895	OAST
Vibration in Planetary Gear Systems	Fred B. Oswald	5258	OAST
Optimized Eddy Current Rotor Damper Analysis	Robert E. Cunningham	6975	OAST
Elastomeric Dampers for Rotating Machinery—Design Handbook	Robert E. Cunningham	6975	OAST
Structural Tailoring of Engine Blades (STAEBL)	Murray S. Hirschbein	272	OAST
Vibration Prediction for Twisted Blades	Gerald V. Brown	380	OAST
Hot, Wet Compression Fatigue Behavior of Composites with Defects	Christos C. Chamis	6831	OAST